# Three-dimensional X-ray Vision by Sparse Tomography

**Samuli Siltanen**

Department of Mathematics and Statistics
University of Helsinki, Finland
samuli.siltanen@helsinki.fi
www.siltanen-research.net

20th European Conference on Mathematics for Industry
Budapest, Hungary, June 19, 2018

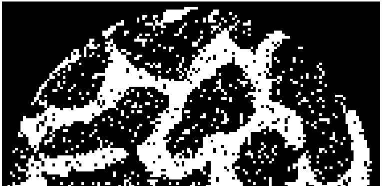

# Finnish Centre of Excellence in Inverse Modelling and Imaging

2018-2025

ACADEMY OF FINLAND

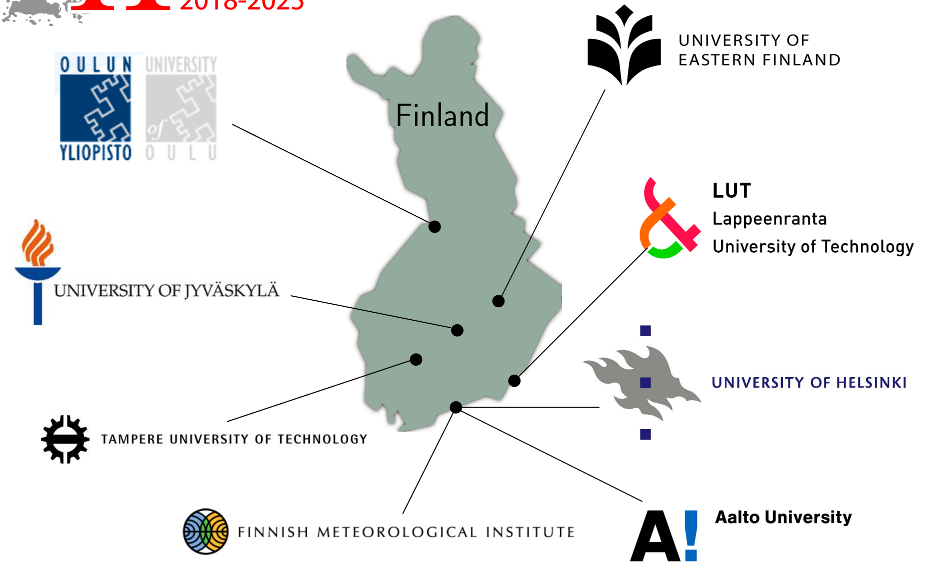

# This my industrial-academic background

- 2009: Professor, University of Helsinki, Finland
- 2006: Professor, Tampere University of Technology, Finland
- 2005: R&D scientist at Palodex Group
- 2004: R&D scientist at GE Healthcare
- 2002: Postdoc at Gunma University, Japan
- 2000: R&D scientist at Instrumentarium Imaging
- 1999: PhD, Helsinki University of Technology, Finland

# Outline

# X-ray intensity attenuates inside matter, here shown with a homogeneous block

https://www.youtube.com/watch?v=IfXo2S1xXCQ

## Here is a more complicated example: a 2D slice through a human head

Andrew Ciscel, Wikimedia commons

## Now the attenuation process is more complicated because there are different tissues

https://youtu.be/lvUAOeS1sv8

# After calibration we are observing how much attenuating matter the X-ray encounters in total

https://youtu.be/RFArLtWEfsQ

## This sweeping movement is the data collection mode of first-generation CT scanners

https://youtu.be/JHUz5oyeZb0

# Modern CT scanners look like this


Wikimedia commons

# Modern scanners rotate at high speed

https://commons.wikimedia.org/wiki/File:CT-Rotation.ogv

Hellerhoff & Markwitz, Wikimedia commons

# This is the inverse problem of tomography: we only know the data

https://youtu.be/pr8bXB0oAqI

# This is an illustration of the standard reconstruction by filtered back-projection

https://youtu.be/tRD58IO1FKw

# Godfrey Hounsfield and Allan McLeod Cormack developed X-ray tomography

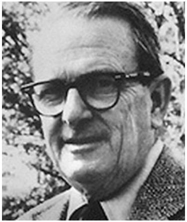

Hounsfield (top) and Cormack received Nobel prizes in 1979.

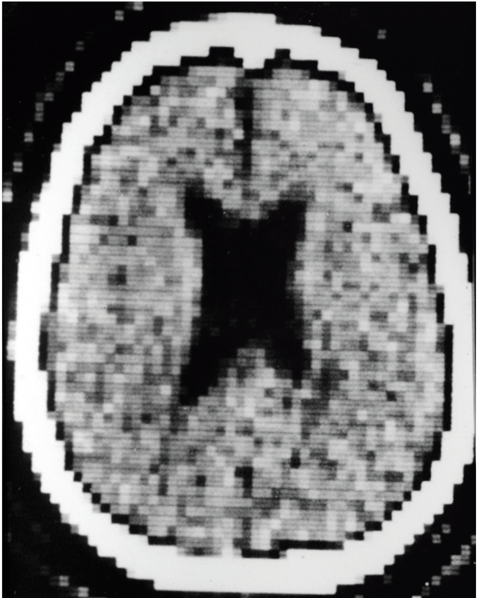

# Reconstruction of a function from its line integrals was first invented by Johann Radon in 1917

Johann Radon (1887-1956)

$$f(P) = -\frac{1}{\pi}\int_0^\infty \frac{d\overline{F_p}(q)}{q}$$

# Diagnosing stroke with X-ray tomography

Ischemic stroke

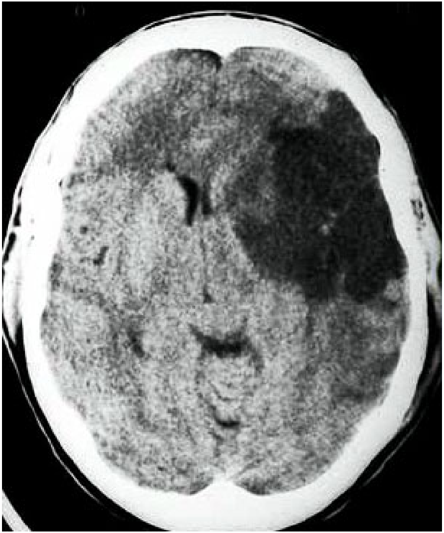

CT image from Jansen 2008

Hemorrhagic stroke

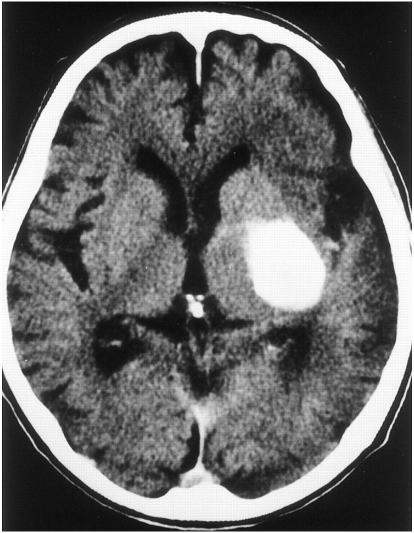

CT image from Nakano *et al.* 2001

# Tomography: case closed?

# Outline

# We collected X-ray projection data of a walnut from 1200 directions

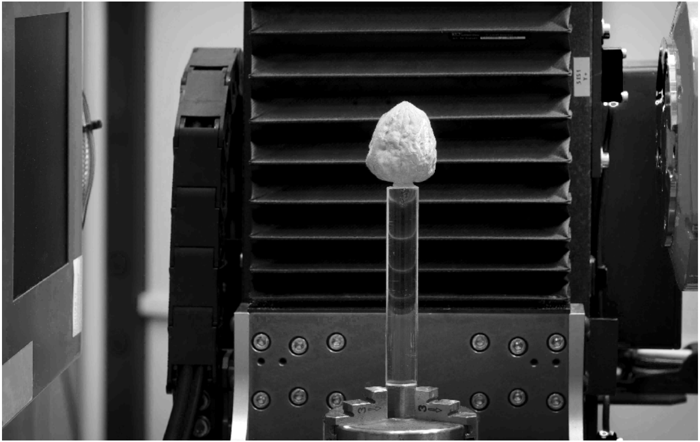

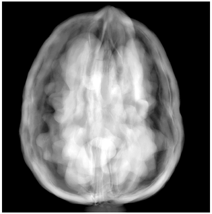

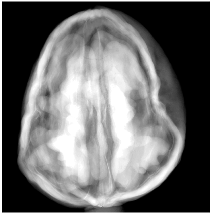

Laboratory and data collection by Keijo Hämäläinen and Aki Kallonen, University of Helsinki.

The data is openly available at http://fips.fi/dataset.php, thanks to Esa Niemi and Antti Kujanpää

# Reconstructions of a 2D slice through the walnut using filtered back-projection (FBP)

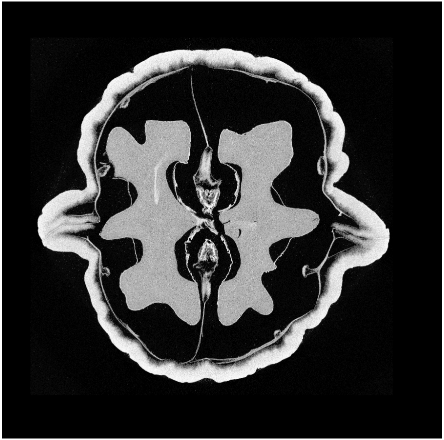

FBP with comprehensive data
(1200 projections)

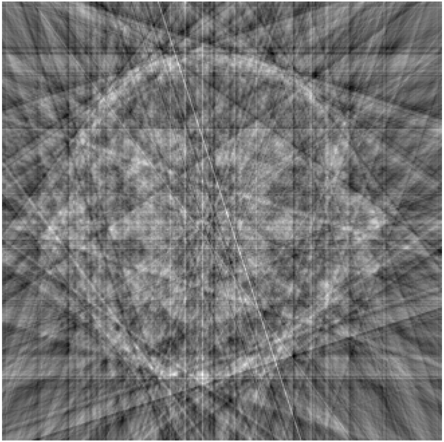

FBP with sparse data
(20 projections)

# Sparse-data reconstruction of the walnut using non-negative total variation regularization

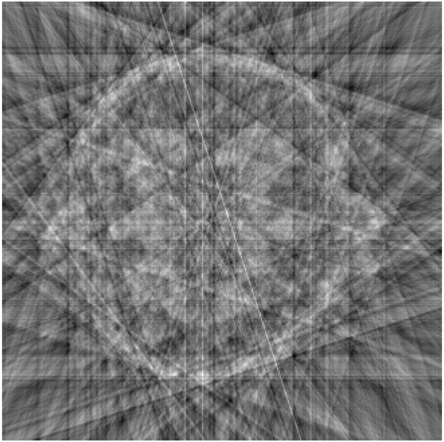

Filtered back-projection

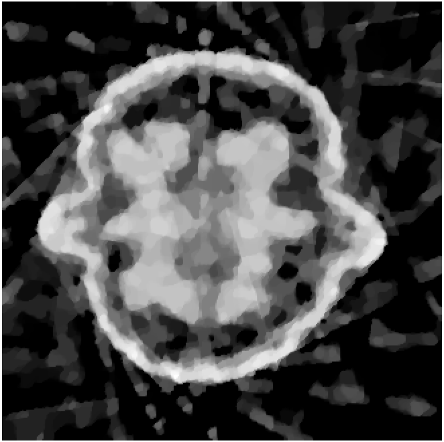

Constrained TV regularization

$$\underset{f\in\mathbb{R}^n_+}{\arg\min}\left\{\|Af-m\|_2^2+\alpha\|\nabla f\|_1\right\}$$

## TV tomography: $\arg\min_{f \in \mathbb{R}^n} \{\|Af - m\|_2^2 + \alpha \|\nabla f\|_1\}$

**1992** Rudin, Osher & Fatemi: denoise images by taking $A = I$
**1998** Delaney & Bresler
**2001** Persson, Bone & Elmqvist
**2003** Kolehmainen, S, Järvenpää, Kaipio, Koistinen, Lassas, Pirttilä & Somersalo (first TV work with measured X-ray data)
**2006** Kolehmainen, Vanne, S, Järvenpää, Kaipio, Lassas & Kalke
**2006** Sidky, Kao & Pan
**2008** Liao & Sapiro
**2008** Sidky & Pan
**2008** Herman & Davidi
**2009** Tang, Nett & Chen
**2009** Duan, Zhang, Xing, Chen & Cheng
**2010** Bian, Han, Sidky, Cao, Lu, Zhou & Pan
**2011** Jensen, Jørgensen, Hansen & Jensen
**2011** Tian, Jia, Yuan, Pan & Jiang
**2012–present:** dozens of articles indicated by Google Scholar

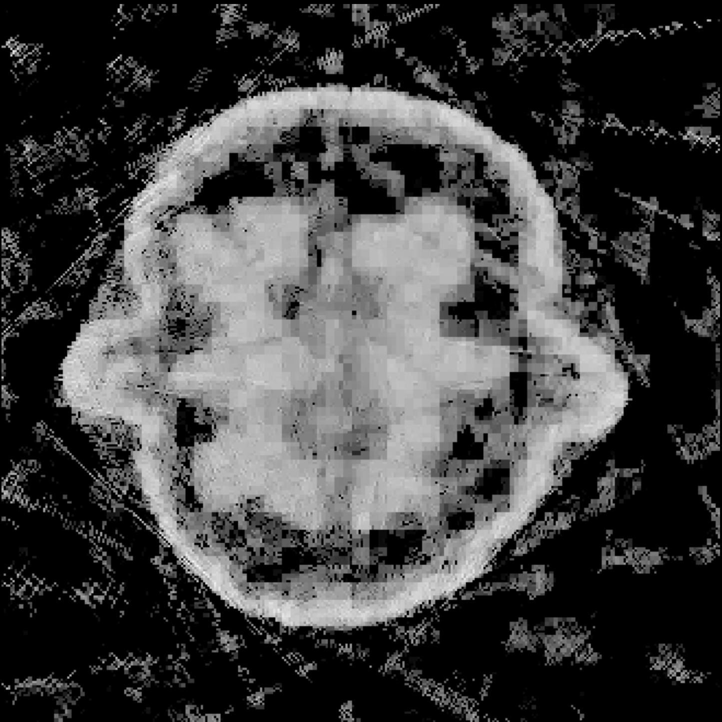

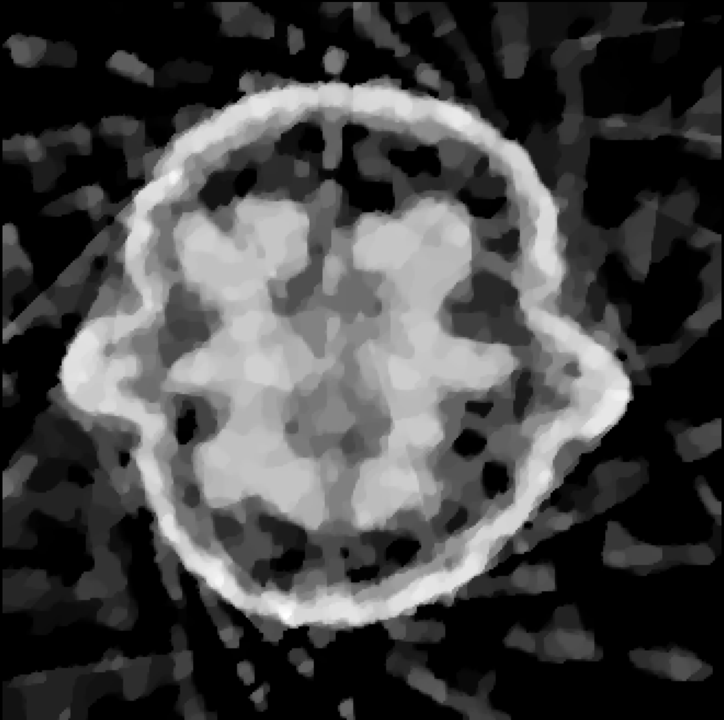

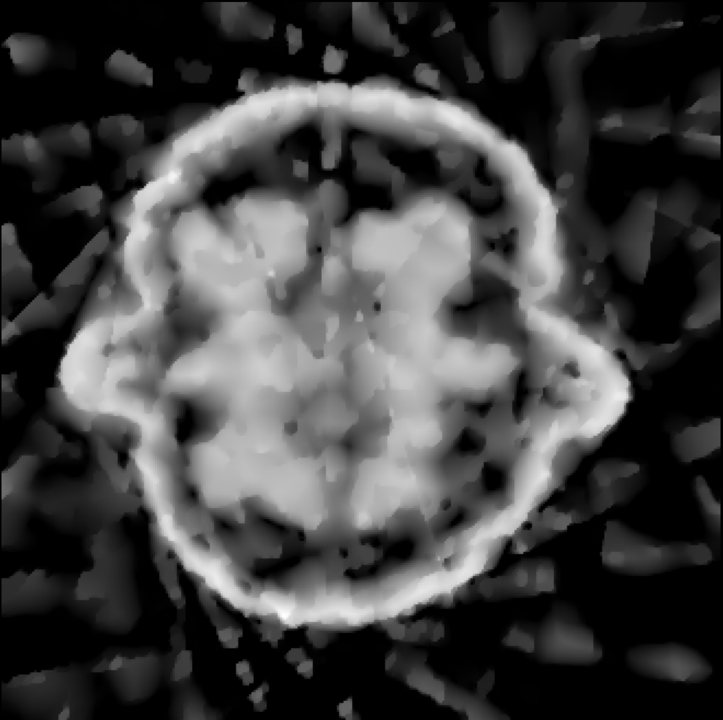

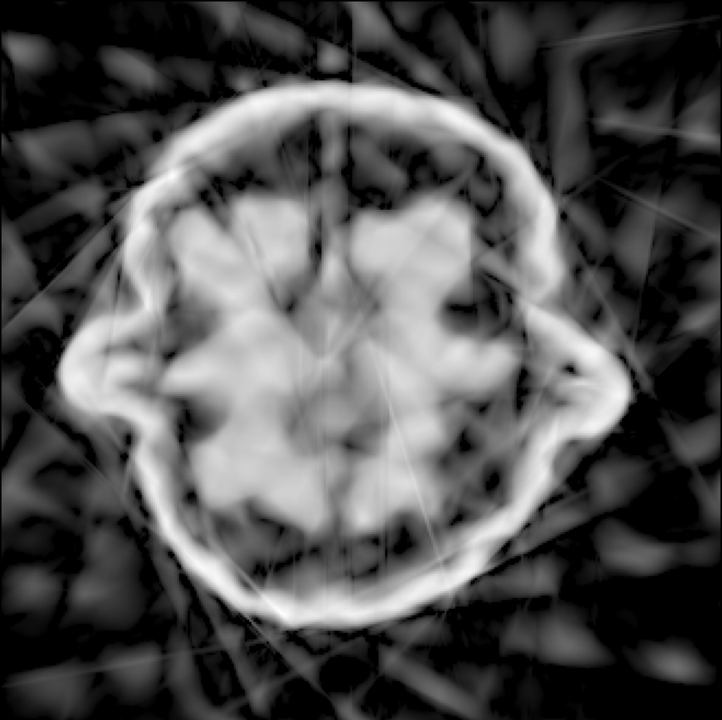

# Outline

- Traditional X-ray tomography
- Tomographic imaging with sparse data
  - Discrete model tor tomography
  - Ill-posedness of the inverse problem
  - Regularization using frame-based sparsity
- Hospital case study: diagnosing osteoarthritis
- Limited angle tomography
- Industrial case study: low-dose 3D dental X-ray imaging
- Industrial case study: welding inspection
- Conclusion

# A projection image is produced by parallel X-rays and several detector pixels (here three pixels)

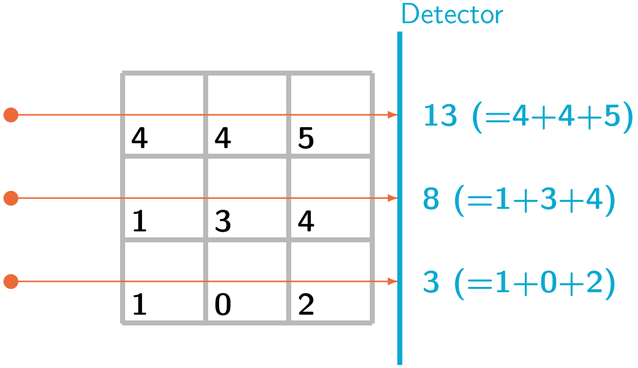

## For tomographic imaging it is essential to record projection images from different directions

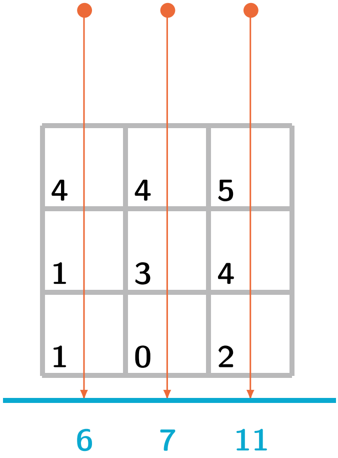

## The length of X-rays traveling inside each pixel is important, thus here the square roots

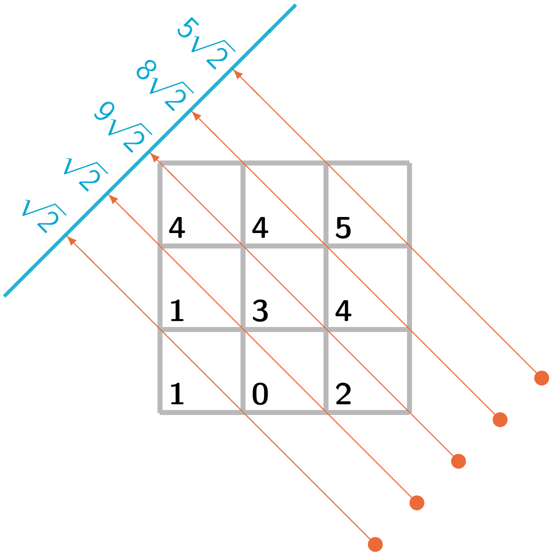

# The direct problem of tomography is to find the projection images from known tissue

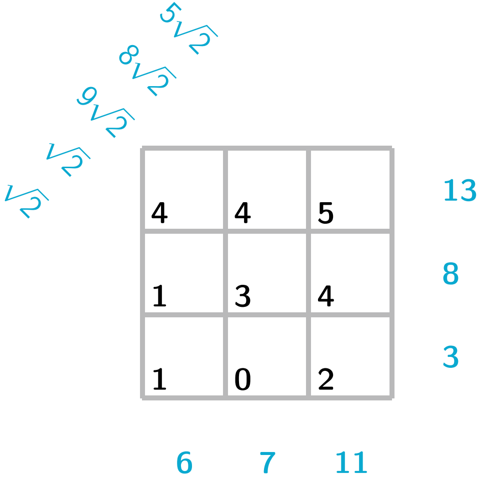

# The inverse problem of tomography is to reconstruct the interior from X-ray data

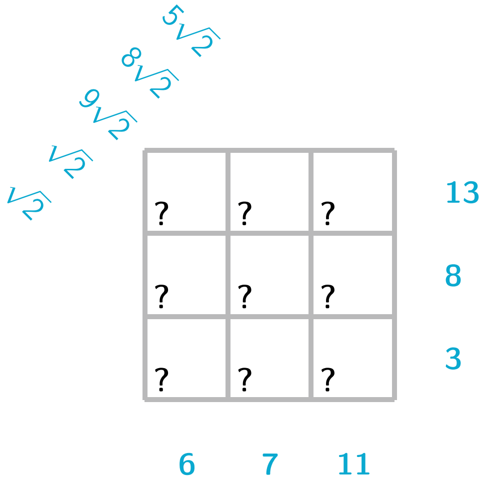

# The limited-angle problem is harder than the full-angle problem

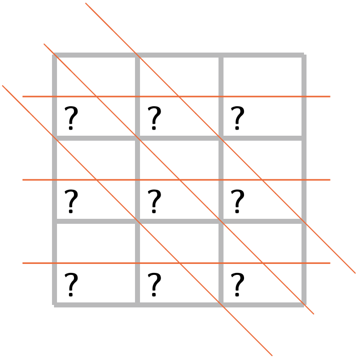


9 unknowns,
6 equations

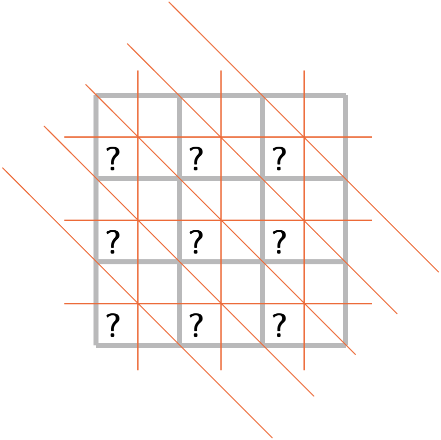


9 unknowns,
11 equations

# In limited-angle imaging, different objects may produce the same data

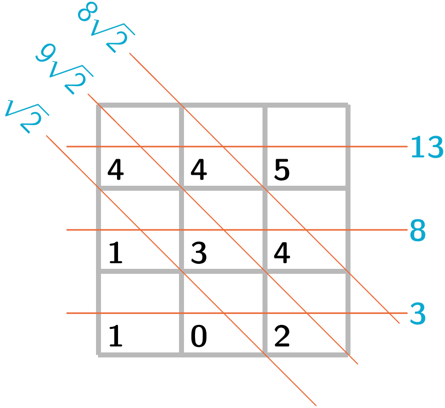


Mathematically this means that the matrix $A$ has nontrivial kernel.

| | | |
|---|---|---|
| 5 | 6 | 2 |
| 1 | 5 | 2 |
| 4 | 0 | -1 |

| | | |
|---|---|---|
| 9 | 1 | 3 |
| 1 | 0 | 7 |
| 3 | 0 | 0 |

## We write the reconstruction problem in matrix form

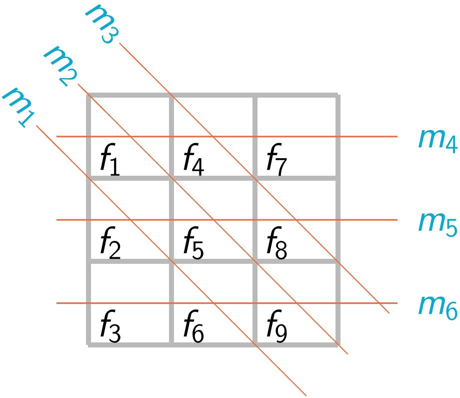


$$f = \begin{bmatrix} f_1 \\ f_2 \\ f_3 \\ f_4 \\ f_5 \\ f_6 \\ f_7 \\ f_8 \\ f_9 \end{bmatrix}, \quad m = \begin{bmatrix} m_1 \\ m_2 \\ m_3 \\ m_4 \\ m_5 \\ m_6 \end{bmatrix},$$

Measurement model: $m = Af + \varepsilon$

## This is the matrix equation related to the above measurement

$$\begin{bmatrix} m_1 \\ m_2 \\ m_3 \\ m_4 \\ m_5 \\ m_6 \end{bmatrix} = \begin{bmatrix} 0 & \sqrt{2} & 0 & 0 & 0 & \sqrt{2} & 0 & 0 & 0 \\ \sqrt{2} & 0 & 0 & 0 & \sqrt{2} & 0 & 0 & 0 & \sqrt{2} \\ 0 & 0 & 0 & \sqrt{2} & 0 & 0 & 0 & \sqrt{2} & 0 \\ 1 & 0 & 0 & 1 & 0 & 0 & 1 & 0 & 0 \\ 0 & 1 & 0 & 0 & 1 & 0 & 0 & 1 & 0 \\ 0 & 0 & 1 & 0 & 0 & 1 & 0 & 0 & 1 \end{bmatrix} \begin{bmatrix} f_1 \\ f_2 \\ f_3 \\ f_4 \\ f_5 \\ f_6 \\ f_7 \\ f_8 \\ f_9 \end{bmatrix} + \begin{bmatrix} \varepsilon_1 \\ \varepsilon_2 \\ \varepsilon_3 \\ \varepsilon_4 \\ \varepsilon_5 \\ \varepsilon_6 \end{bmatrix}$$

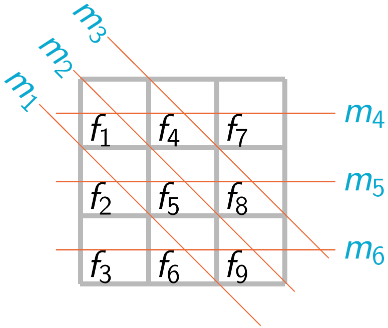

# Outline

## Let us construct a more complicated example

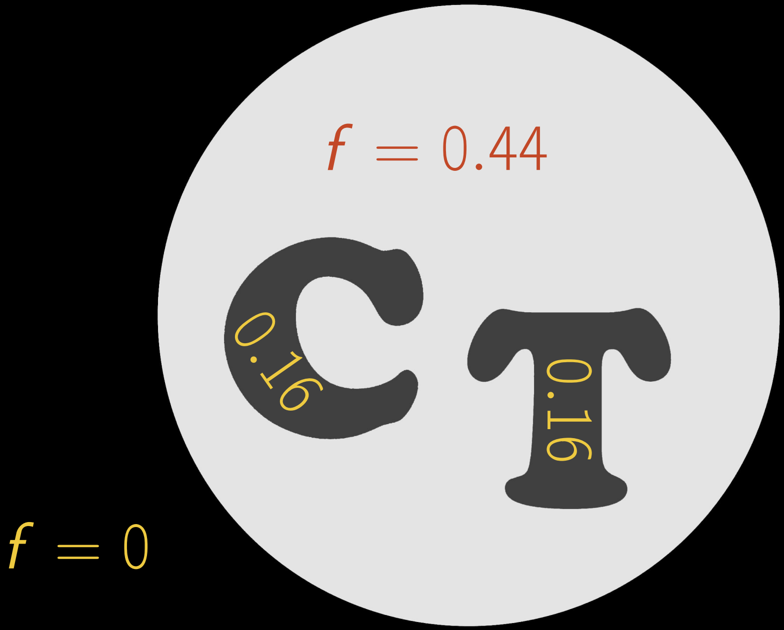

# Discretize the unknown by dividing it into pixels


Target (unknown)

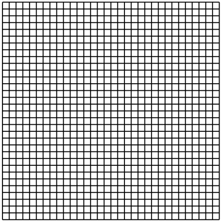

32×32 pixel grid

# System matrix $A$, given by the grid and X-rays

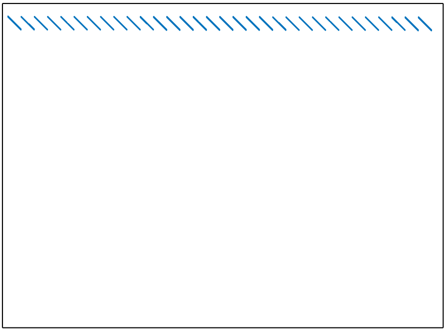

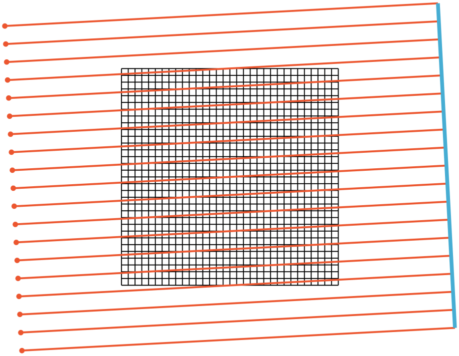

$735 \times 1024$ system matrix $A$, only nonzero elements shown

$32 \times 32$ pixel grid

# System matrix $A$, given by the grid and X-rays

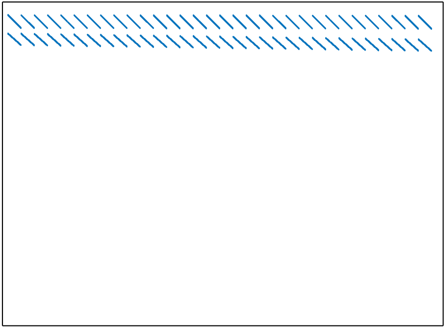

$735 \times 1024$ system matrix $A$,
only nonzero elements shown

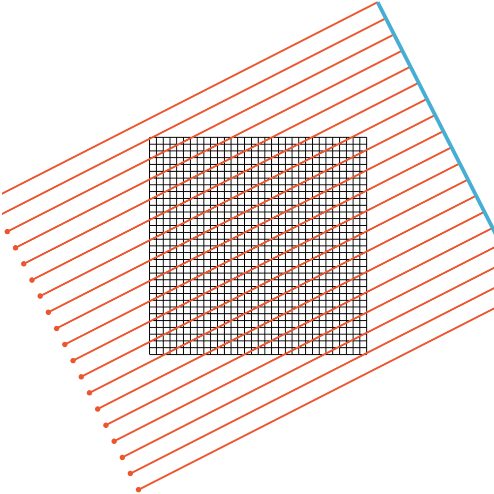

$32 \times 32$ pixel grid

# System matrix $A$, given by the grid and X-rays

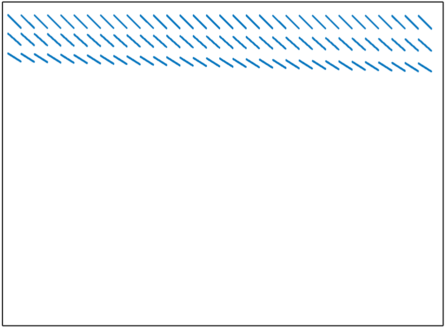

$735 \times 1024$ system matrix $A$,
only nonzero elements shown

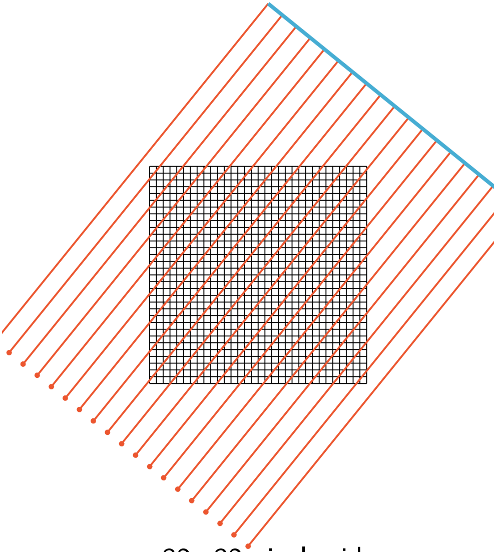

$32 \times 32$ pixel grid

# System matrix $A$, given by the grid and X-rays

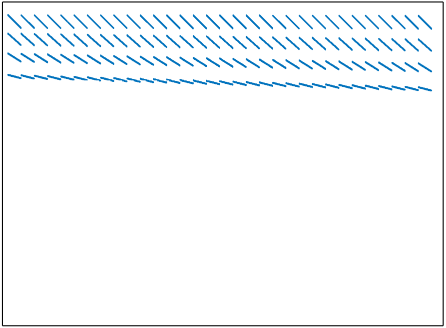

$735 \times 1024$ system matrix $A$,
only nonzero elements shown

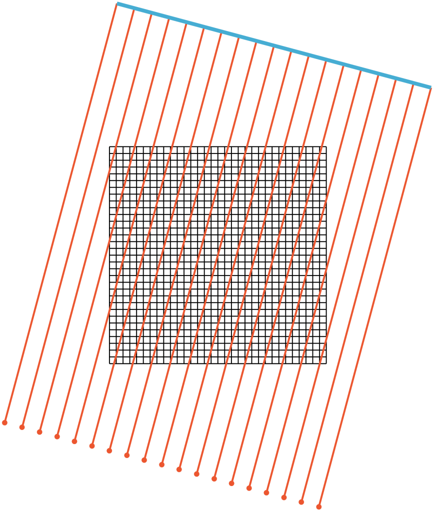

$32 \times 32$ pixel grid

# System matrix $A$, given by the grid and X-rays

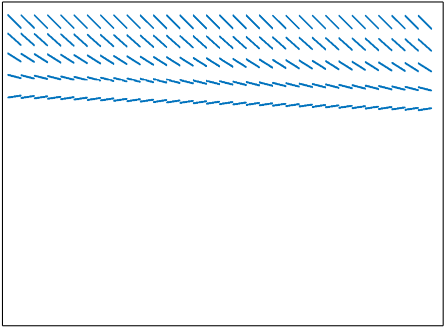

$735 \times 1024$ system matrix $A$,
only nonzero elements shown

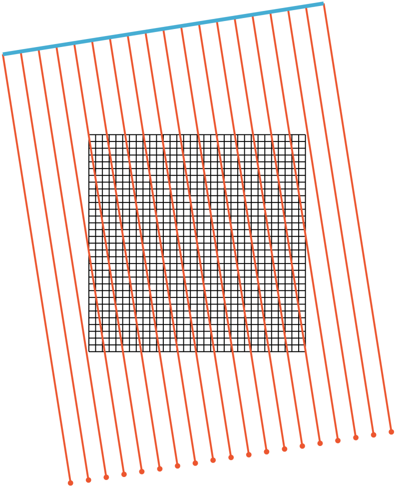

$32 \times 32$ pixel grid

# System matrix $A$, given by the grid and X-rays

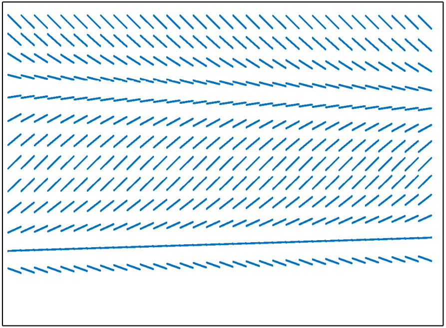

735×1024 system matrix $A$, only nonzero elements shown

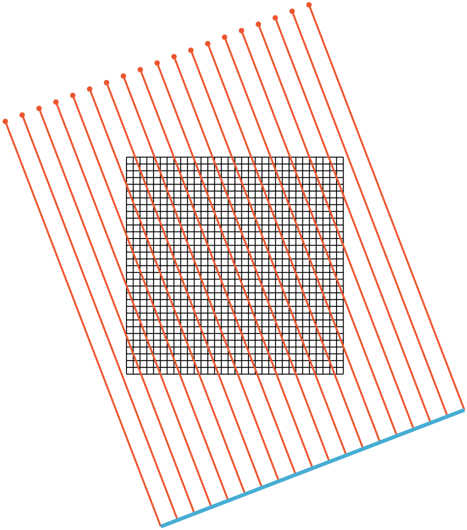

32×32 pixel grid

# System matrix $A$, given by the grid and X-rays

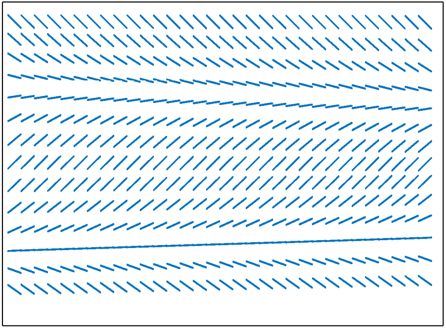

$735\times1024$ system matrix $A$, only nonzero elements shown

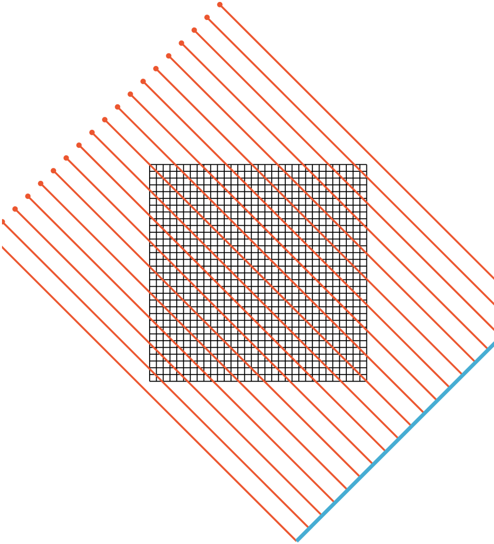

$32\times32$ pixel grid

# System matrix $A$, given by the grid and X-rays

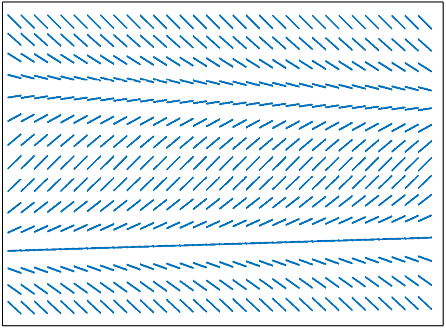

735×1024 system matrix $A$,
only nonzero elements shown

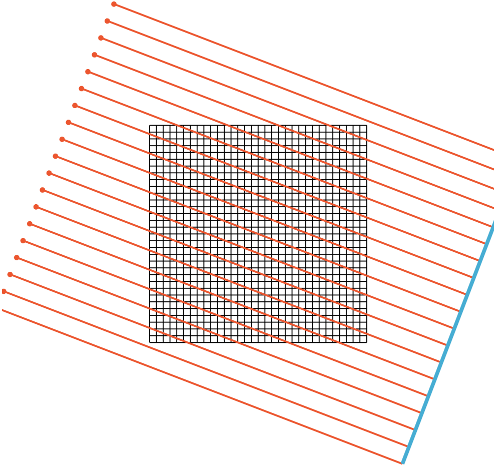

32×32 pixel grid

## What can we expect to see from sparse data?

Object

$\xrightarrow{\quad A \quad}$

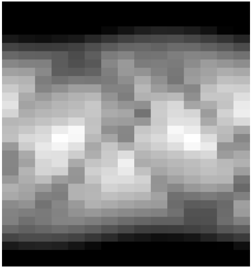

Sinogram

THEOREM 4.2. *A finite set of radiographs tells nothing at all.*

For some reason this theorem provokes merriment. It is so plainly one of those mathematical ideals untainted by any possibility of practical application.

[Cormack 1963], [Smith, Solmon & Wagner 1977, Theorem 4.2]

# Naive reconstruction using the minimum norm solution from the normal equation $(A^T A)f^\dagger = A^T m$

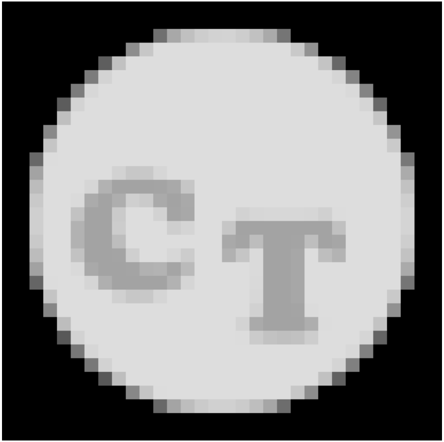

Original phantom, values between zero (black) and 0.44

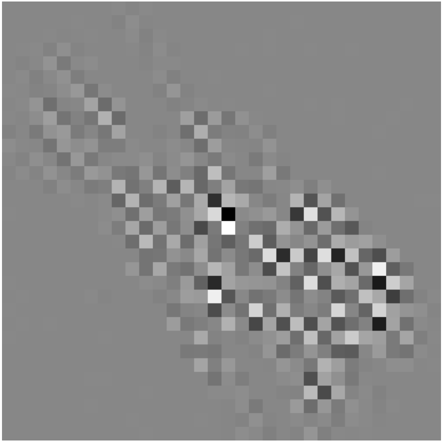

Reconstruction: minimum pixel value $-1.5 \cdot 10^{14}$, maximum value $1.3 \cdot 10^{14}$

# Naive reconstruction using the minimum norm solution with non-negativity constraint

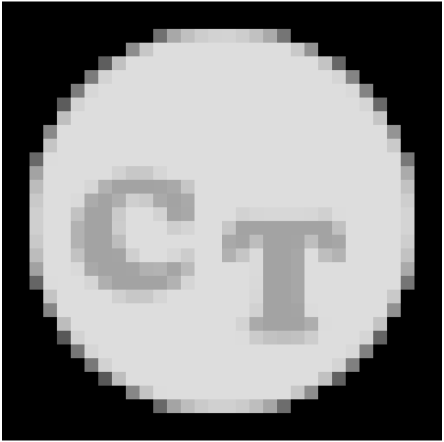

Original phantom, values between zero (black) and 0.44

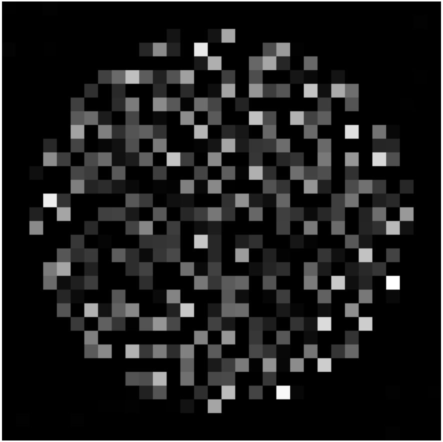

Reconstruction: minimum value 0, maximum value 2.3

# Illustration of the ill-posedness of sparse tomography

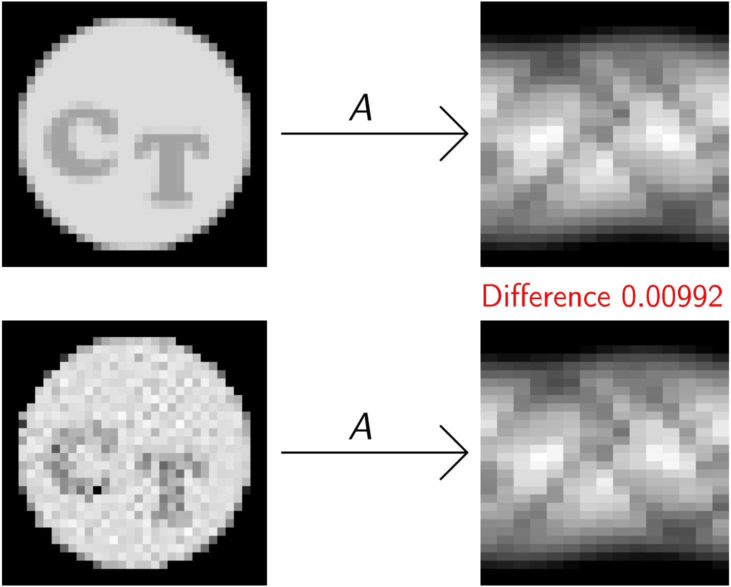

# Illustration of the ill-posedness of sparse tomography

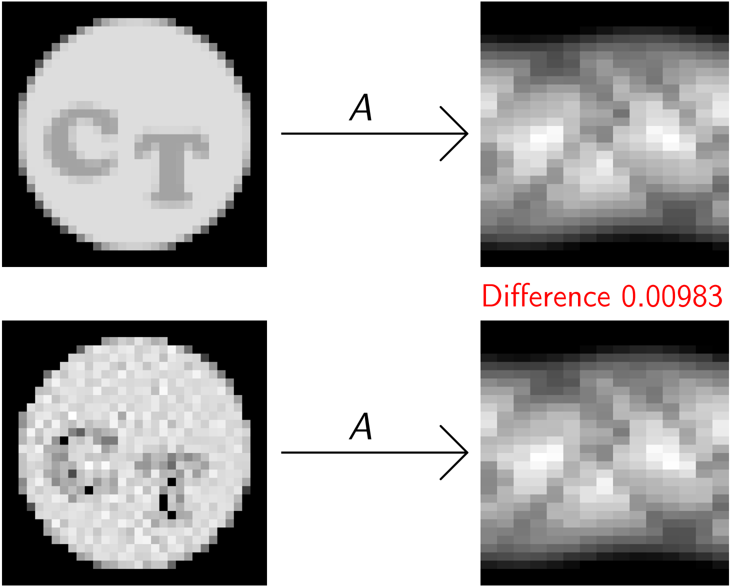

# Singular value decomposition $A = U^T D V$

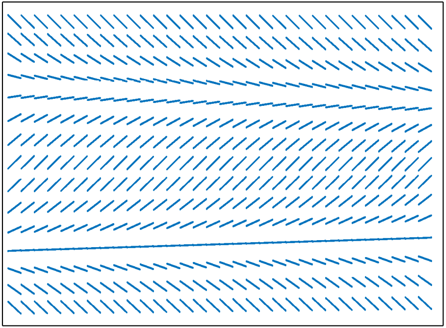

$735 \times 1024$ system matrix $A$, only nonzero elements shown

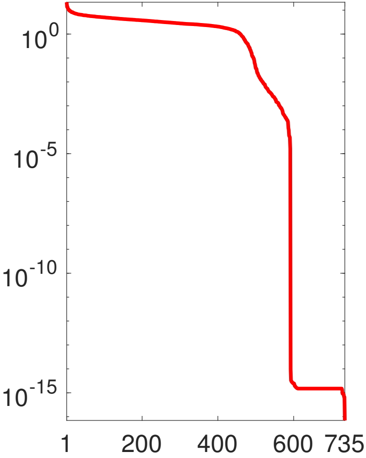


Singular values of $A$ (diagonal of $D$)

# Outline

# Daubechies, Defrise and de Mol introduced a revolutionary inversion method in 2004

Consider the sparsity-promoting variational regularization

$$\arg\min_{f\in\mathbb{R}^n} \left\{ \|Af - m\|_2^2 + \mu \|Wf\|_1 \right\},$$

where $W$ is an orthonormal wavelet transform. The minimizer can be computed using the iteration

$$f_{j+1} = W^{-1} S_\mu W \left( f_j + A^T(m - Af_j) \right),$$

where the soft-thresholding operation

$$S_\mu(x) = \begin{cases} x + \frac{\mu}{2} & \text{if } x \leq -\frac{\mu}{2}, \\ 0 & \text{if } |x| < \frac{\mu}{2}, \\ x - \frac{\mu}{2} & \text{if } x \geq \frac{\mu}{2}, \end{cases}$$

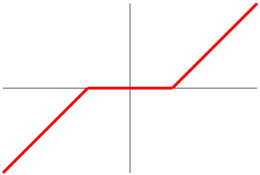

is applied to each wavelet coefficient separately.

# We modify the method so that non-negativity constraint has rigorous mathematical foundation

The minimizer

$$\operatorname*{argmin}_{f \in \mathbb{R}^n_+} \left\{ \frac{1}{2} \|Af - m\|_2^2 + \mu \, \|Wf\|_1 \right\}$$

can be computed using this iteration:

$$\begin{aligned}
y^{(i+1)} &= \mathbb{P}_C\Big(f^{(i)} - \tau \nabla g(f^{(i)}) - \lambda W^T v^{(i)}\Big) \\
v^{(i+1)} &= \Big(I - S_\mu\Big)\Big(W y^{(i+1)} + v^{(i)}\Big) \\
f^{(i+1)} &= \mathbb{P}_C\Big(f^{(i)} - \tau \nabla g(f^{(i)}) - \lambda W^T v^{(i+1)}\Big)
\end{aligned}$$

where $\tau > 0$, $\lambda > 0$ and $g(f) = \frac{1}{2}\|Af - m\|_2^2$. Here $\mathbb{P}_C$ denotes projection to the non-negative "quadrant."

[Loris & Verhoeven 2011], [Chen, Huang & Zhang 2016]

# Illustration of the Haar wavelet transform

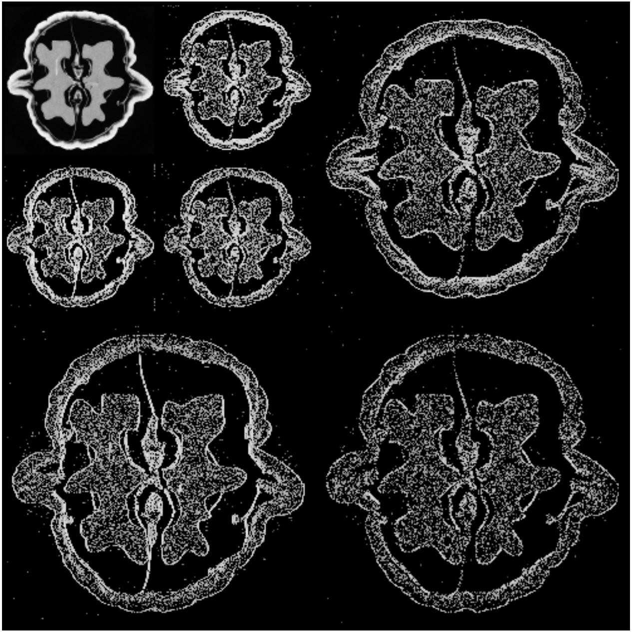

# Sparse-data reconstruction of the walnut using Haar wavelet sparsity

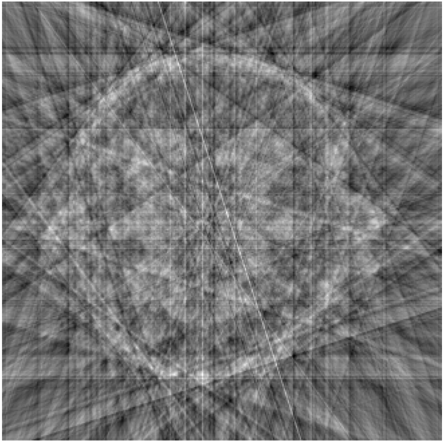

Filtered back-projection

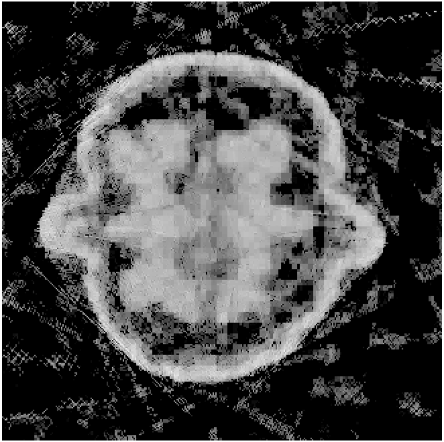

Constrained Besov regularization

$$\arg\min_{f \in \mathbb{R}^n_+} \left\{ \|Af - m\|_2^2 + \alpha \|f\|_{B^1_{11}} \right\}$$

# How to choose the thresholding parameter $\mu$? Here it is too small.

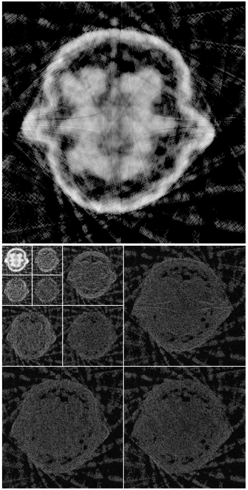

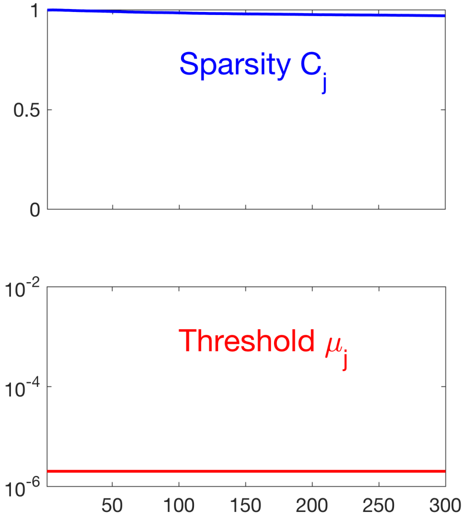

# How to choose the thresholding parameter $\mu$? Here it is too large.

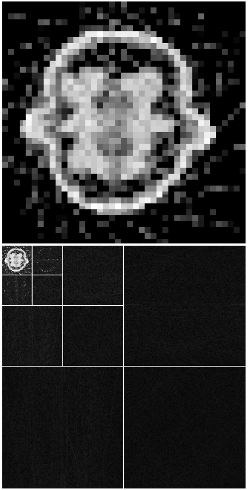

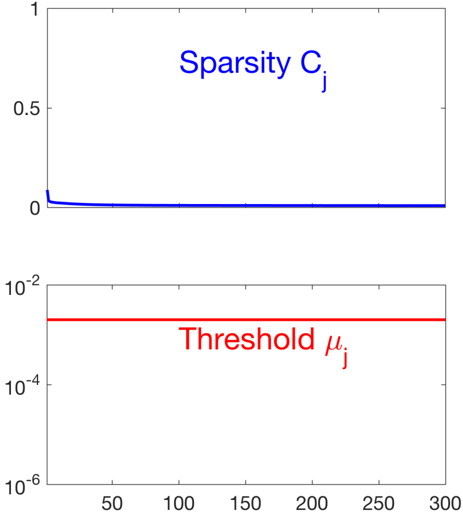

# Automatic parameter choice using controlled wavelet-domain sparsity (CWDS)

Assume given the *a priori* sparsity level $0 \le \mathcal{C}_{\text{pr}} \le 1$.
Denote by $\mathcal{C}_j$ the sparsity of the $j$th iterate $f_j \in \mathbb{R}^n$:

$$\mathcal{C}_j = (\text{number of nonzero elements in } Wf_j \in \mathbb{R}^n)/n.$$

The CWDS iteration is based on proportional-integral-derivative (PID) controllers:

$$\mu^{(i+1)} = \mu^{(i)} + \beta(\mathcal{C}^{(i)} - \mathcal{C}_{\text{pr}}).$$

[Purisha, Rimpeläinen, Bubba & S 2018]

# CWDS choice of the thresholding parameter $\mu$

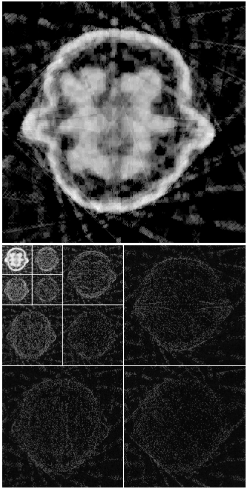

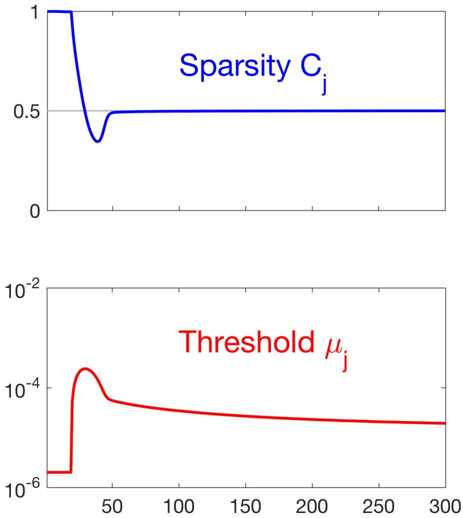

# CWDS choice of the thresholding parameter $\mu$

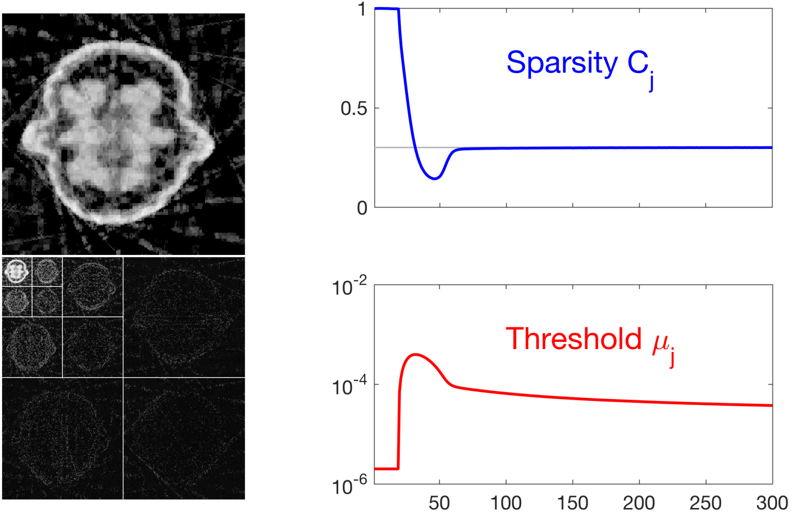

# Outline

# This is a joint work with

**Tatiana Bubba**, University of Helsinki, Finland

**Sakari Karhula**, Oulu University Hospital, Finland

**Juuso Ketola**, Oulu University Hospital, Finland

**Maximilian März**, TU Berlin

**Miika T. Nieminen**, University of Oulu, Finland

**Zenith Purisha**, University of Helsinki, Finland

**Juho Rimpeläinen**, University of Helsinki, Finland

**Simo Saarakkala**, Oulu University Hospital, Finland

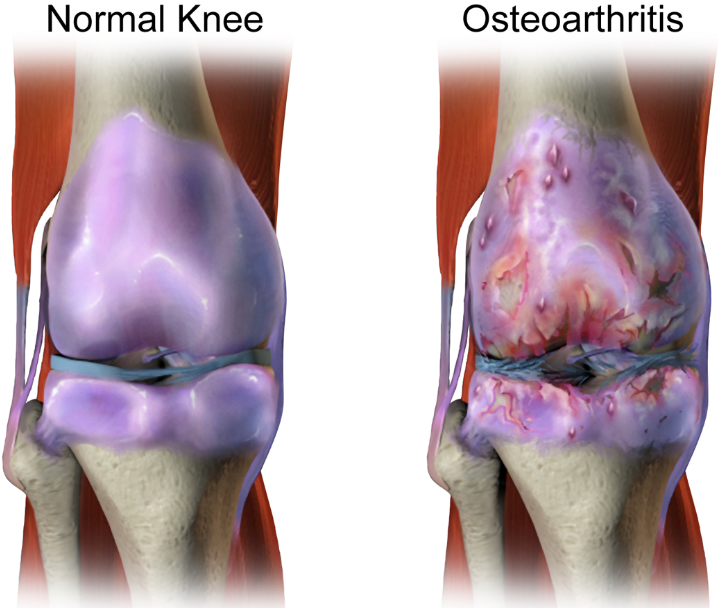
Normal Knee
Osteoarthritis

# We consider small specimens of human bone imaged using microtomography

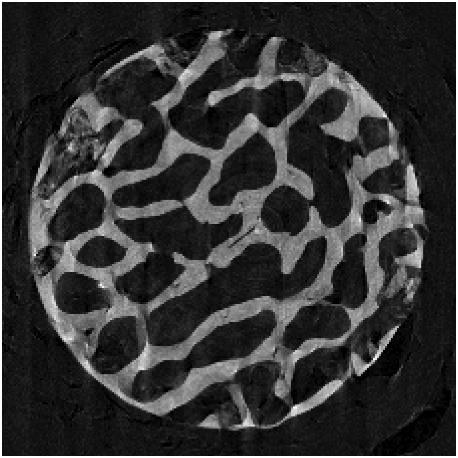

Slice of 3D reconstruction by FDK based on **596 angles**

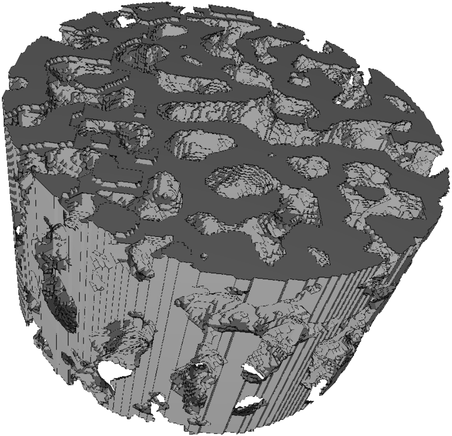

Three-dimensional structure

# We pick out a smaller region of interest for osteoarthritis analysis

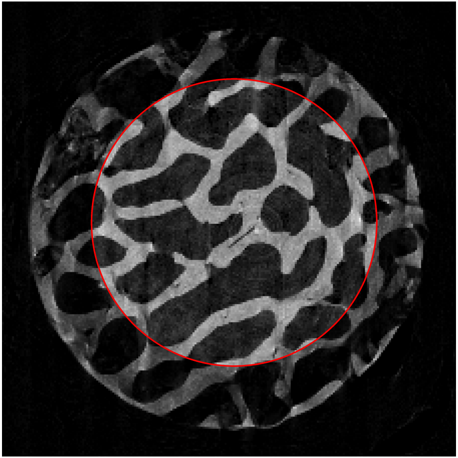

Slice of 3D reconstruction by FDK based on **596 angles**

Slice of 3D region of interest after binary thresholding

# We use two numerical quality measures applied to segmented three-dimensional bone structure

Trabecular thickness

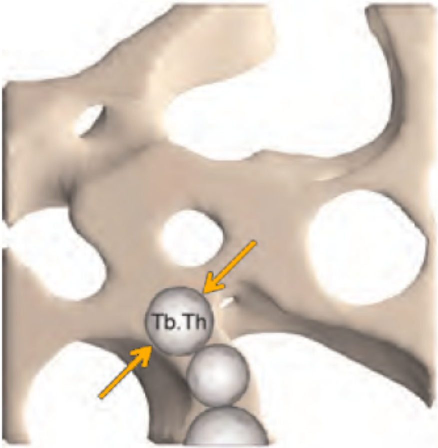


Trabecular separation

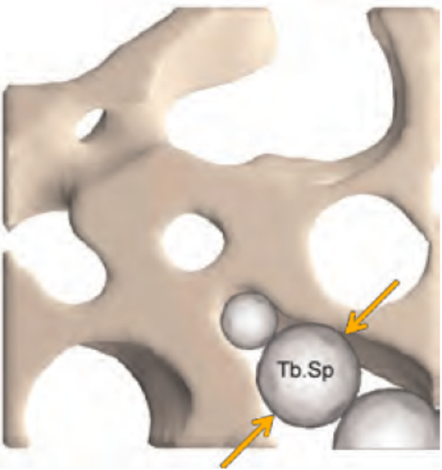


[Bouxsein, Boyd, Christiansen, Guldberg, Jepsen, & Müller 2010]

# The goal is to reduce measurement time by recording fewer radiographs

3D FDK reconstruction
based on **40 angles**

3D shearlet-sparsity reconstruction
based on **40 angles**

# Bone quality parameters from ground truth

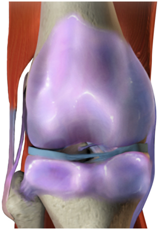

Projections: 300

**Thickness** **0.34**

**Separation** **0.71**

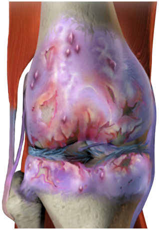

Projections: 300

**Thickness** **0.37**

**Separation** **0.35**

[Purisha, Karhula, Rimpeläinen, Nieminen, Saarakkala & S, submitted]

# Results from FDK reconstructions

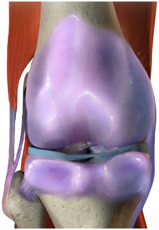

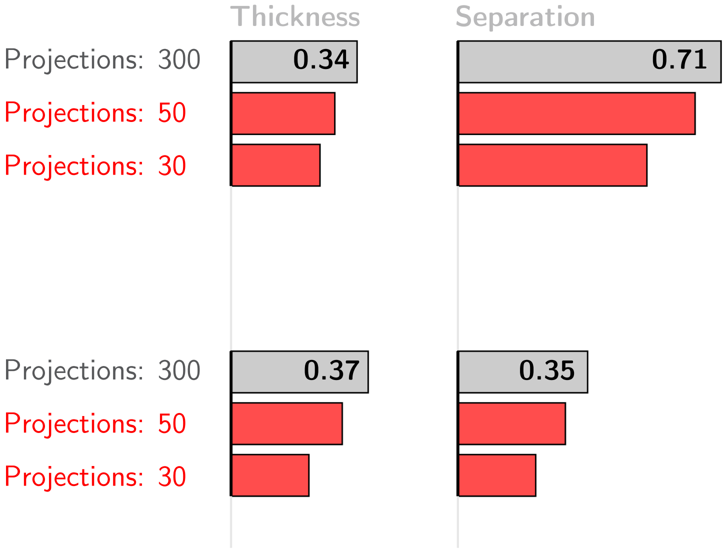


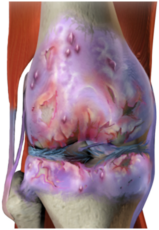

[Purisha, Karhula, Rimpeläinen, Nieminen, Saarakkala & S, submitted]

# Results from 3D shearlet-sparsity reconstructions

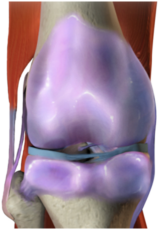

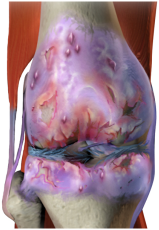

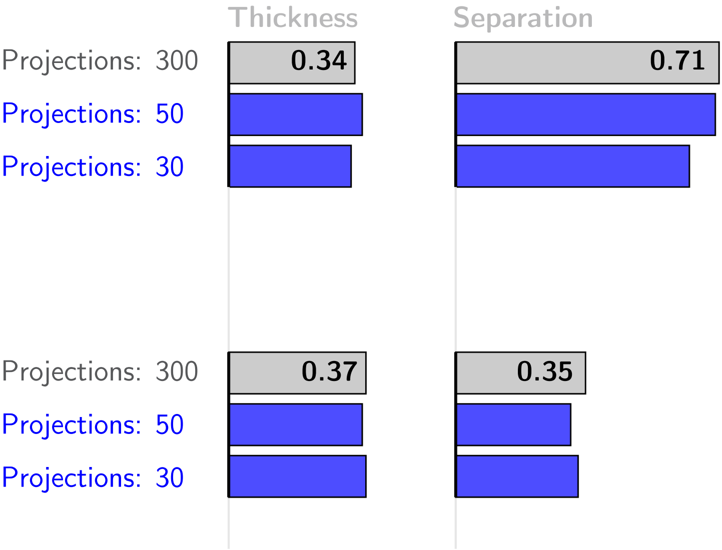


[Purisha, Karhula, Rimpeläinen, Nieminen, Saarakkala & S, submitted]

# Outline

# Construction of limited-angle sinogram

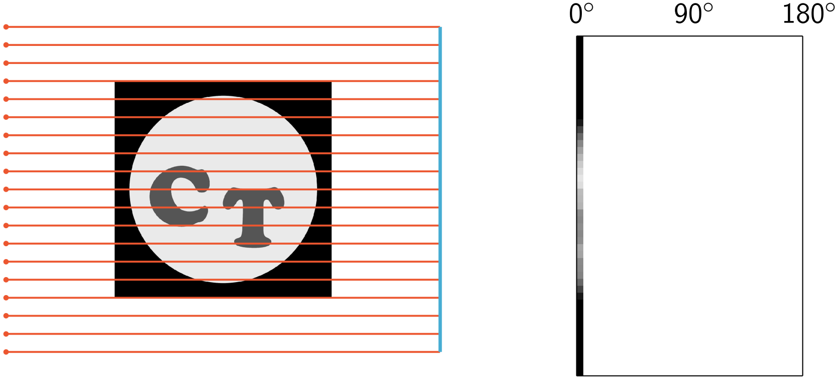

# Construction of limited-angle sinogram

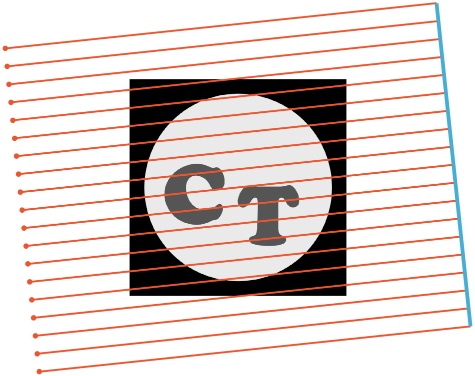

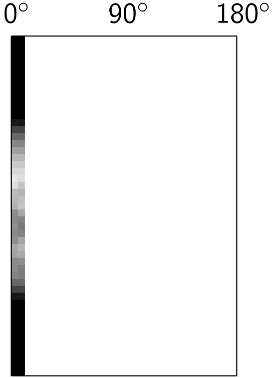

# Construction of limited-angle sinogram

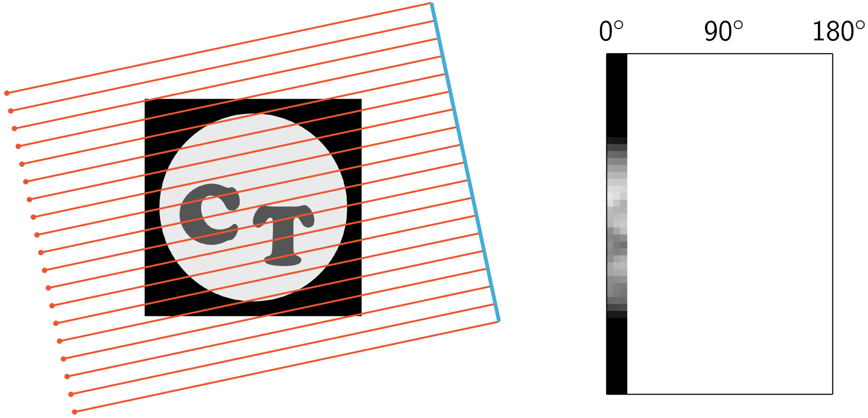

# Construction of limited-angle sinogram

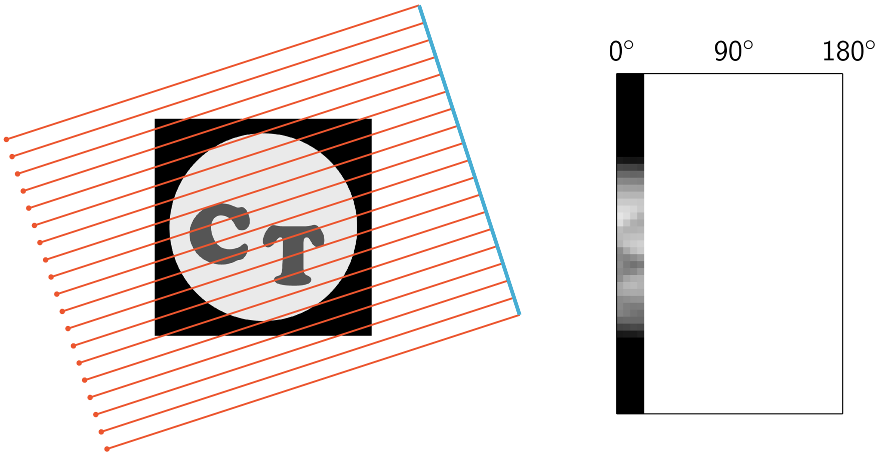

# Construction of limited-angle sinogram

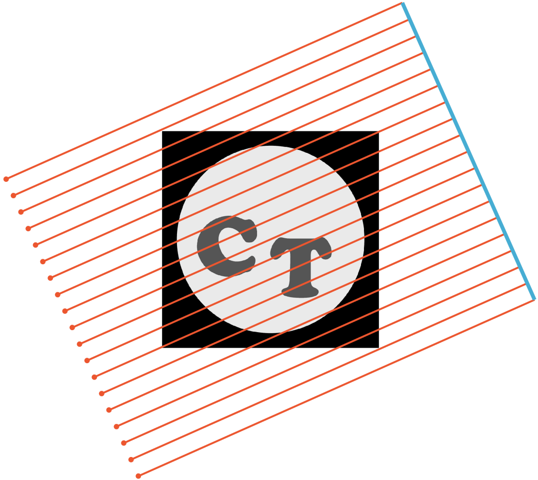

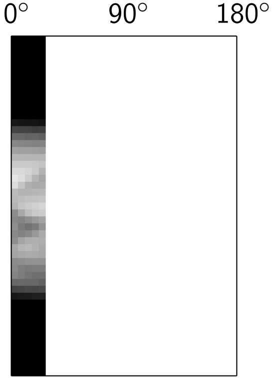

# Construction of limited-angle sinogram

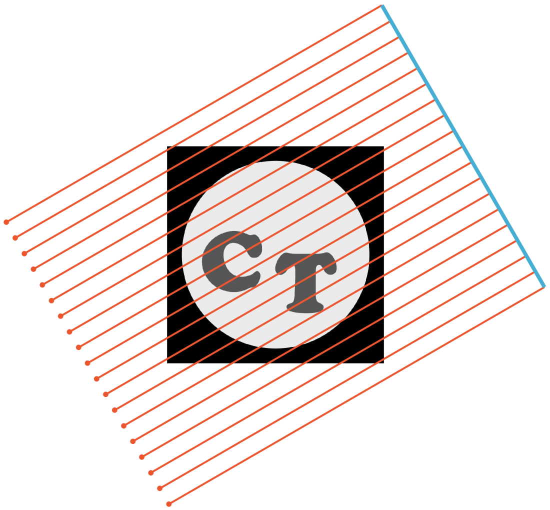


# Construction of limited-angle sinogram

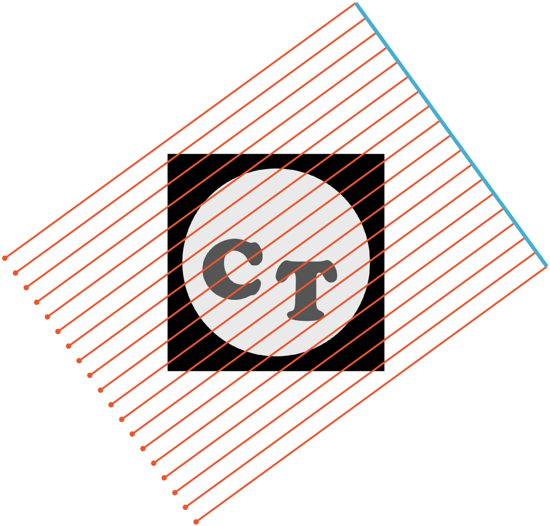


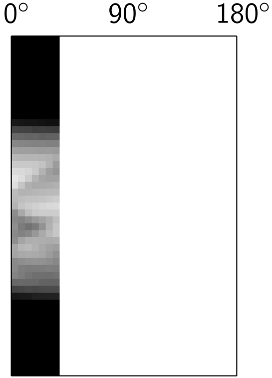

# Construction of limited-angle sinogram

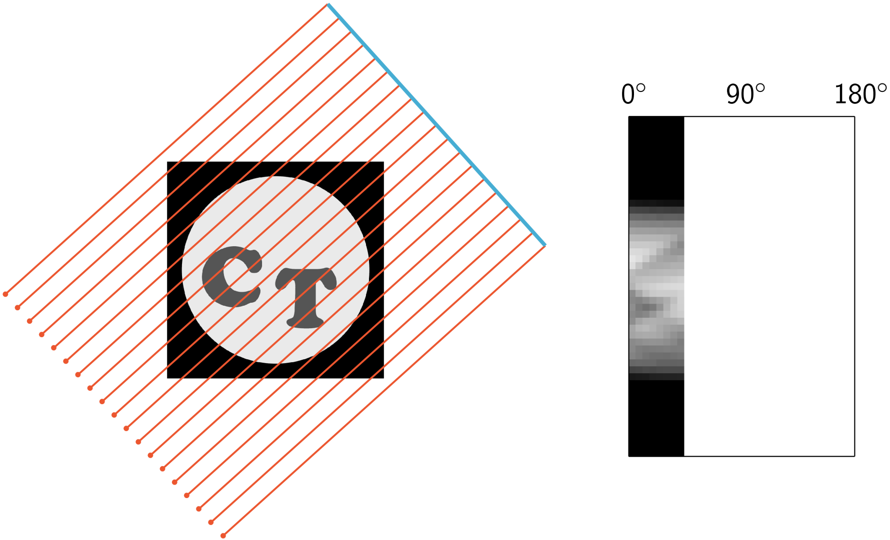

# Construction of limited-angle sinogram

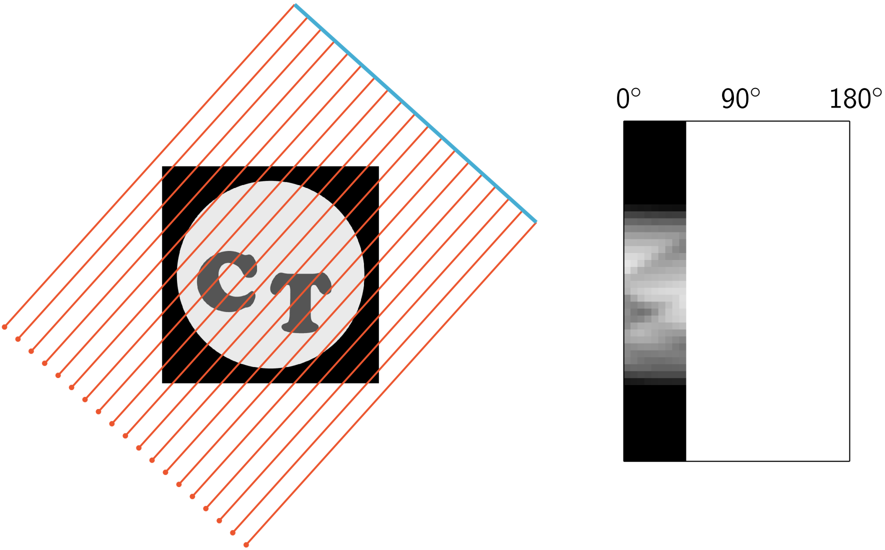

# Construction of limited-angle sinogram

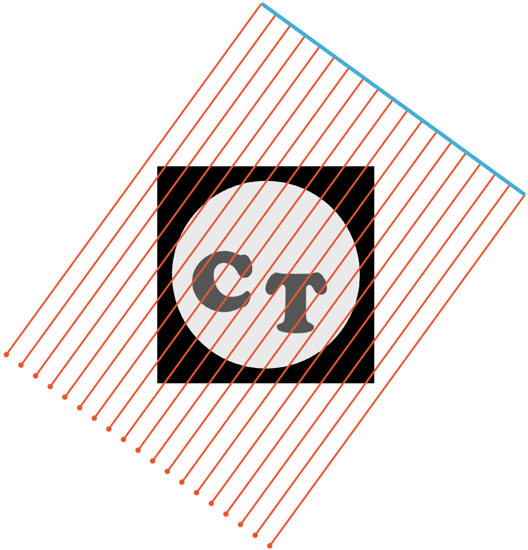

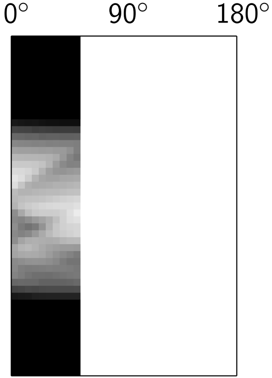

# Construction of limited-angle sinogram

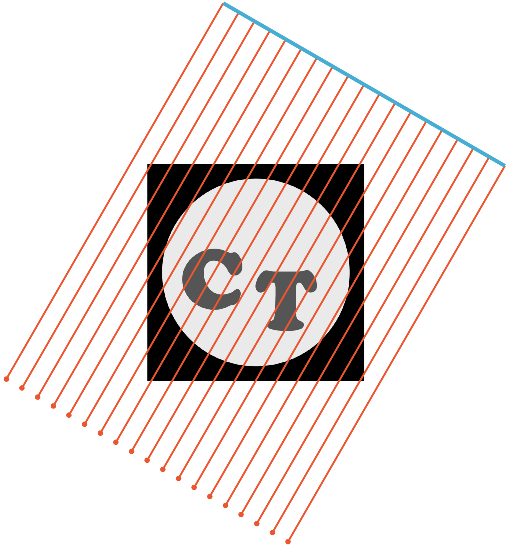

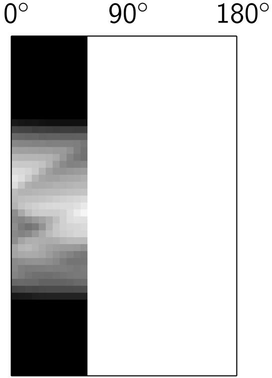

# Construction of limited-angle sinogram

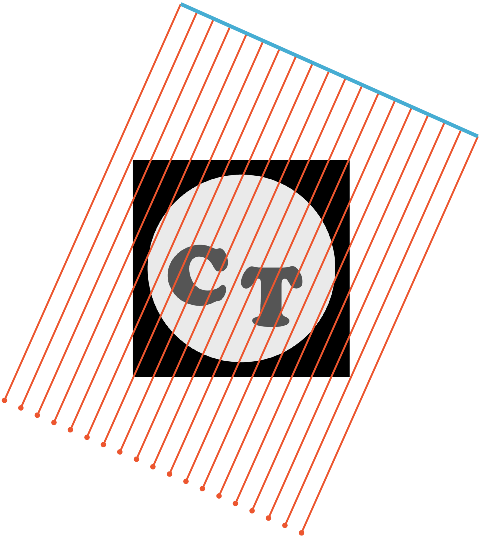


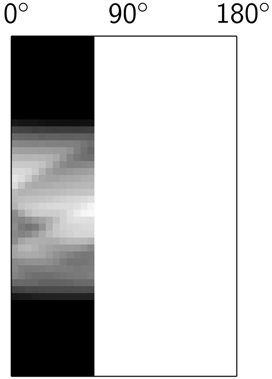

# Construction of limited-angle sinogram

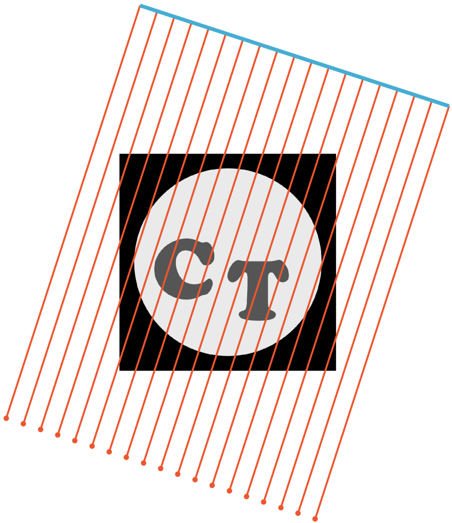

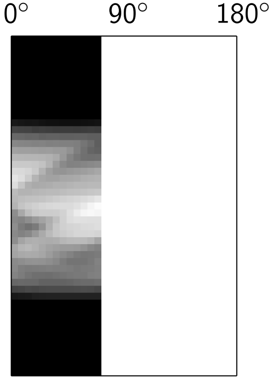

# Construction of limited-angle sinogram

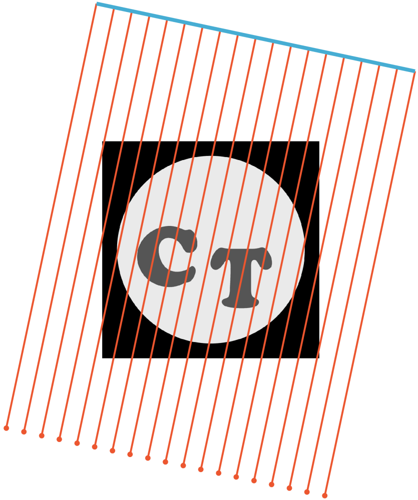


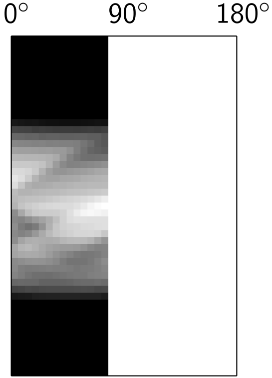

# Construction of limited-angle sinogram

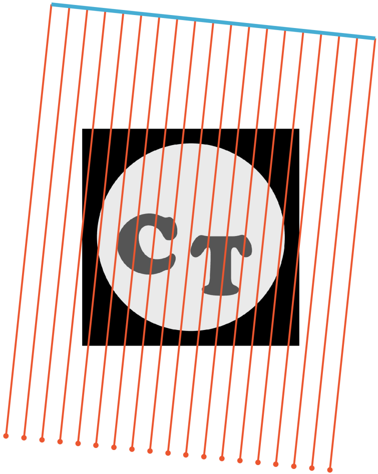


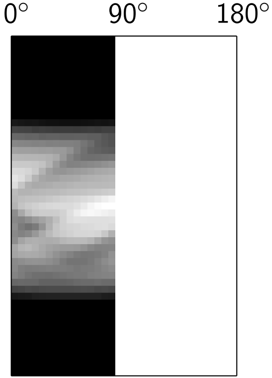

# SVD reveals the ill-posedness of the limited-angle problem, see Davison 1983 and Louis 1986

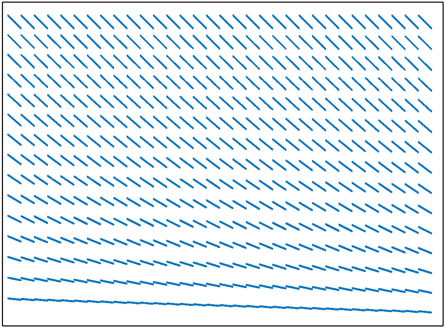

735×1024 system matrix $A$,
only nonzero elements shown

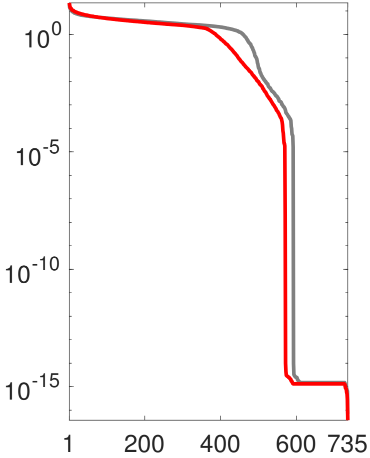


Singular values of $A$
(diagonal of $D$)

# Limited data gives only part of the wavefront set

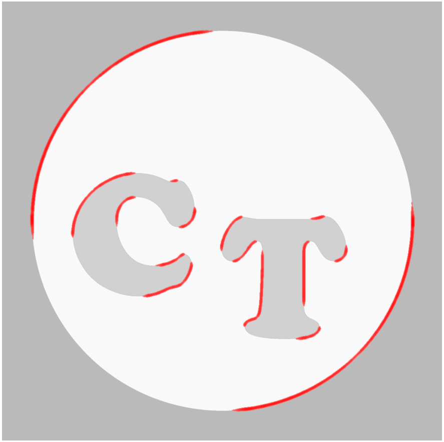


Stable part of wavefront set

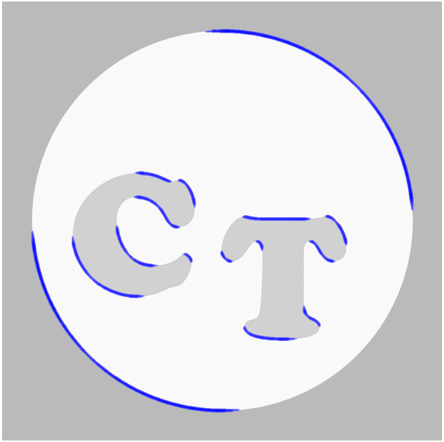


Unstable part of wavefront set

See [Greenleaf & Uhlmann 1989], [Quinto 1993], and [Frikel & Quinto 2013]

# Constrained total variation (TV) regularization

$$\arg\min_{f \in \mathbb{R}^n_+} \left\{ \|Af - m\|_2^2 + \alpha \|\nabla f\|_1 \right\}$$

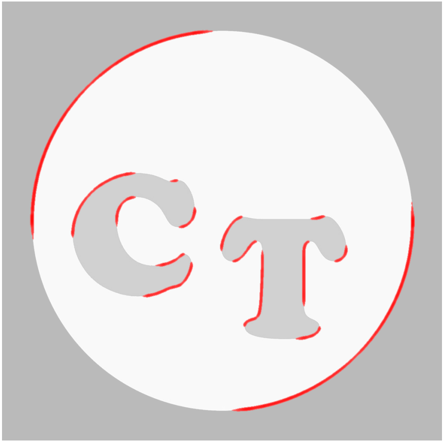


Stable part of wavefront set

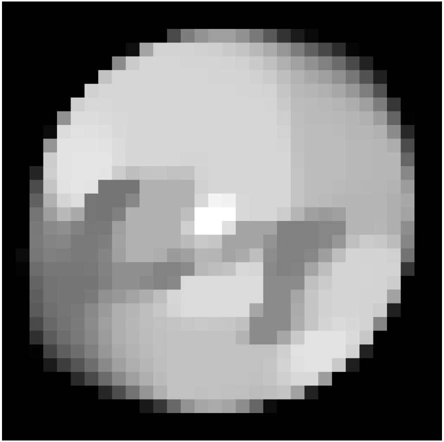

TV regularized reconstruction

# Outline

Traditional X-ray tomography

Tomographic imaging with sparse data
- Discrete model tor tomography
- Ill-posedness of the inverse problem
- Regularization using frame-based sparsity

Hospital case study: diagnosing osteoarthritis

Limited angle tomography

**Industrial case study: low-dose 3D dental X-ray imaging**

Industrial case study: welding inspection

Conclusion

# Application: dental implant planning, where a missing tooth is replaced with an implant

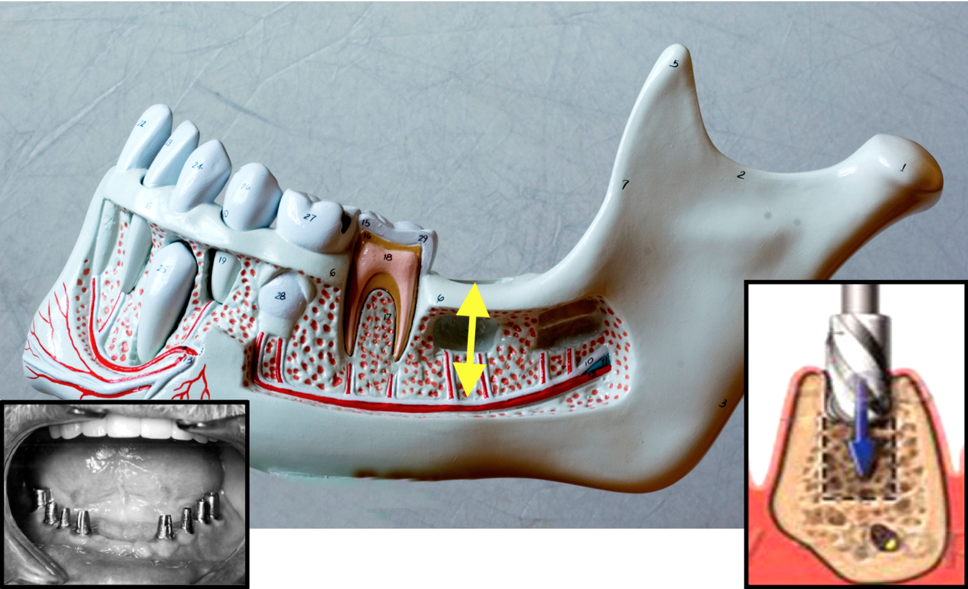

# This is the classical imaging procedure of the panoramic X-ray device

https://www.youtube.com/watch?v=QFTXegPxC4U

# The resulting image shows a sharp layer positioned inside the dental arc

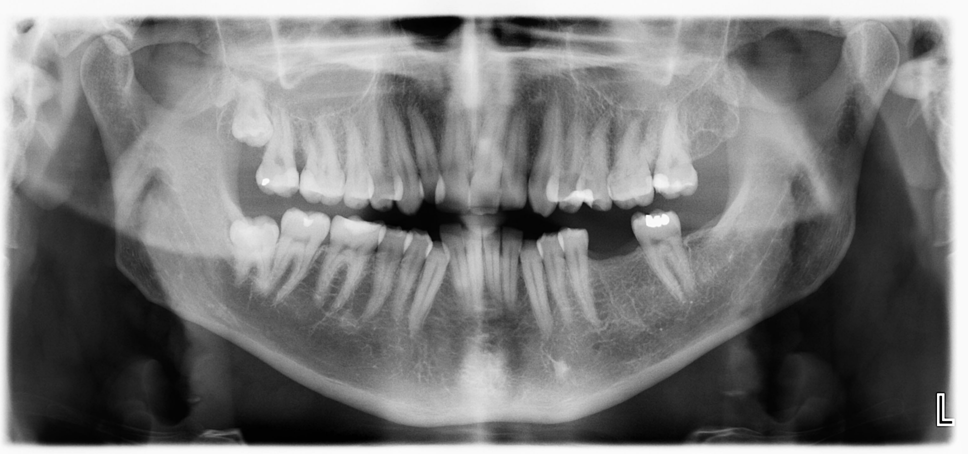

# Nowadays, a digital panoramic imaging device is standard equipment at dental clinics

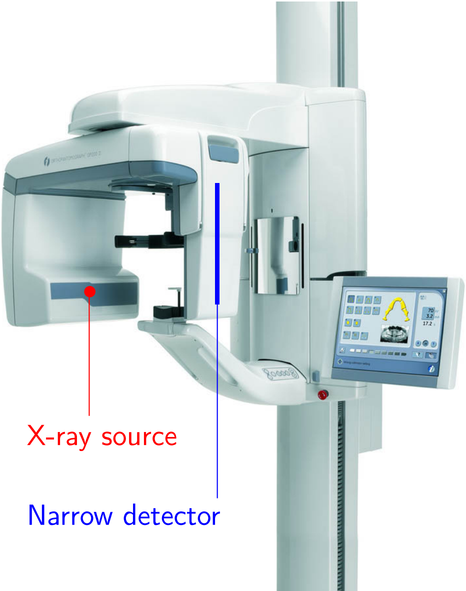


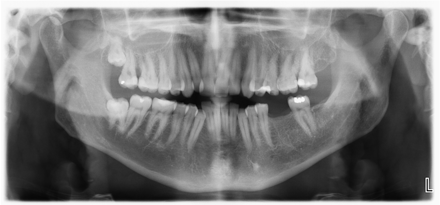

A panoramic dental image offers a general overview showing all teeth and other structures simultaneously.

Panoramic images are not suitable for dental implant planning because of unavoidable geometric distortion.

# We reprogram the panoramic X-ray device so that it collects projection data by scanning

https://www.youtube.com/watch?v=motthjiP8ZQ

# We reprogram the panoramic X-ray device so that it collects projection data by scanning

Number of projection images: **11**

Angle of view: **40 degrees**

Image size: **1000×1000 pixels**

The unknown vector $f$ has **7 000 000** elements.

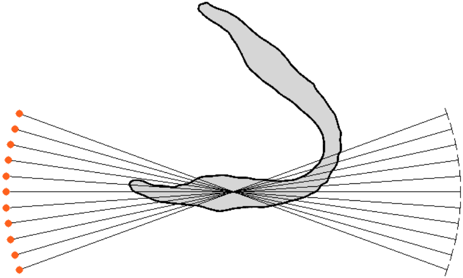

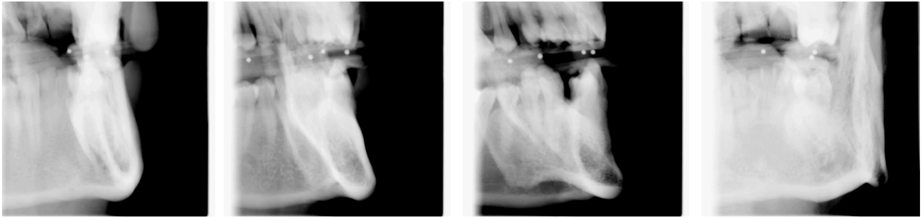

# Standard Cone Beam CT reconstruction delivers 100 times more radiation than VT imaging

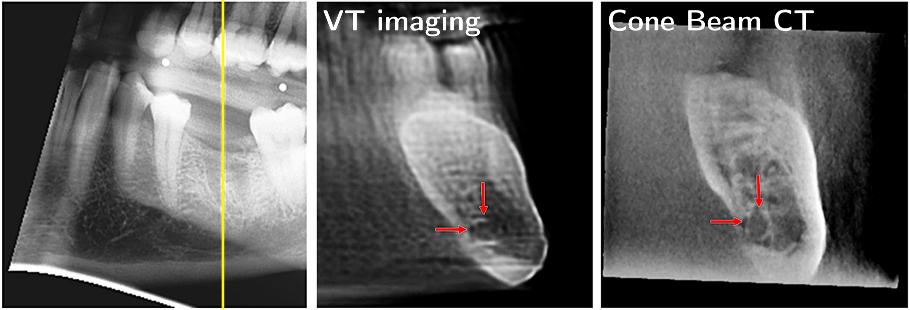


Kolehmainen, Vanne, S, Järvenpää, Kaipio, Lassas & Kalke **2006**

Kolehmainen, Lassas & S **2008**

Cederlund, Kalke & Welander **2009**

Hyvönen, Kalke, Lassas, Setälä & S **2010**

U.S. patent 7269241, thousands of VT units in use

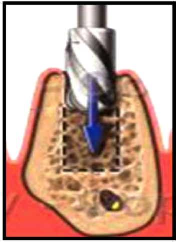

# The VT device was developed in 2001–2012 by

Nuutti Hyvönen
Seppo Järvenpää
Jari Kaipio
Martti Kalke
Petri Koistinen
Ville Kolehmainen
Matti Lassas
Jan Moberg
Kati Niinimäki
Juha Pirttilä
Maaria Rantala
Eero Saksman
Henri Setälä
Erkki Somersalo
Antti Vanne
Simopekka Vänskä
Richard L. Webber

# Outline

# This part is a joint work with

**Alexander Meaney**, University of Helsinki, Finland

**Esa Niemi**, Eniram Ltd., Finland

**Aaro Salosensaari**, University of Helsinki, Finland

**Industrial partners:**

**Kemppi Ltd. (welding tool manufacturer)**

**Ajat Ltd. (X-ray detector manufacturer)**

# Two steel pipes partly welded together

# This is the limited-angle measurement geometry for a narrow CaTd direct conversion detector

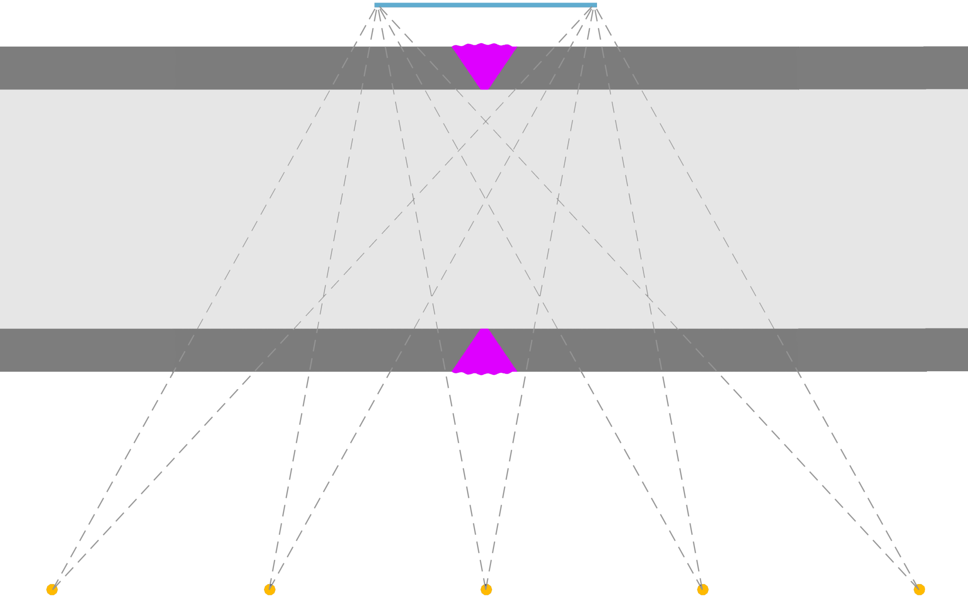

# Reconstruction algorithm: variant of TVR-DART

With a regularization parameter $\alpha > 0$, we minimize

$$\arg\min_{x \in \mathbb{R}^N} \{ \|AS(x) - m\|_2^2 + \alpha TV_\beta(x) \},$$

where $S : \mathbb{R}^N \to \mathbb{R}^N$ is a soft segmentation function given by

$$S(x) = \sum_{g=2}^{G} (\rho_g - \rho_{g-1}) u(x - \tau_g, k_g),$$

with $u(x, k_g) = (1 + e^{-2k_g x})^{-1}$, and $k_g = K/(\rho_g - \rho_{g-1})$. Here $G = 2$ is the number of materials and $3 < K < 6$ is called a transition constant. The parameters $\rho_g$ are the pre-known attenuation values of the materials and $\tau_g$ are the threshold levels between the different attenuations with $\tau_1 = 0$. Above $TV_\beta$ is

$$TV_\beta = \sum_{i,j} \sqrt{(x_{i+1} - x_i)^2 + (x_{i+n} - x_i)^2 + \beta}, \quad \beta > 0.$$

# Reconstruction algorithm: variant of TVR-DART

We mostly follow [Zhuge, Palenstijn & Batenburg 2016] in the implementation of TVR-DART.

However, we make one bigger modification. In this application it makes a huge difference to restrict the degrees of freedom in the domain occupied by the pipe walls.

# Traditional reconstruction by tomosynthesis

Simulated phantom:

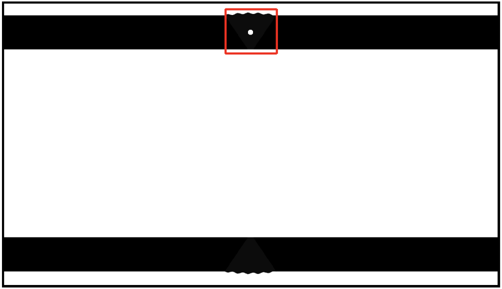

Tomosynthesis:

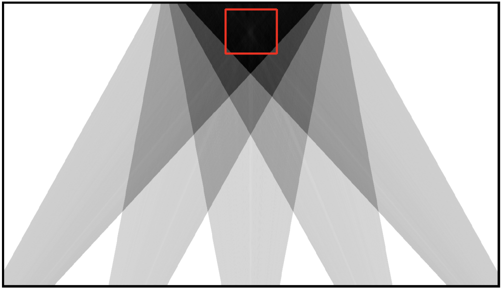

# TVR-DART with domain restriction

Simulated phantom:

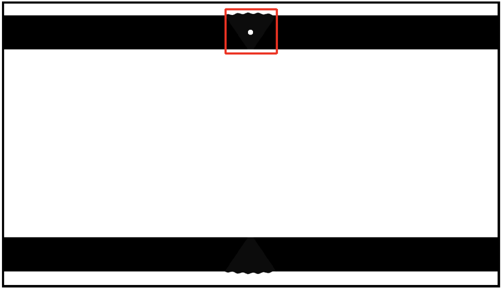

TVR-DART:

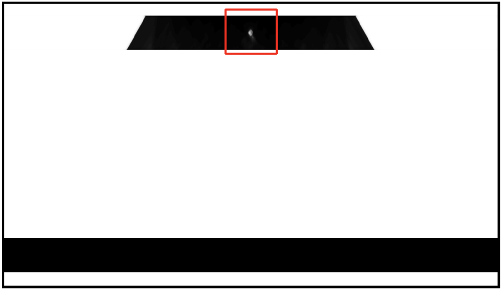

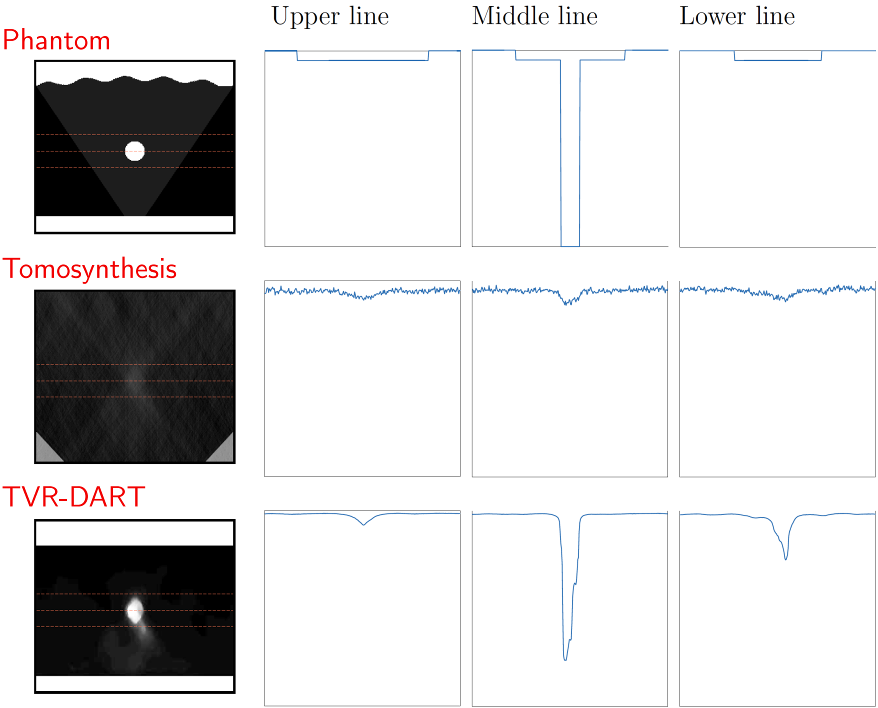
Upper line
Middle line
Lower line
Phantom
Tomosynthesis
TVR-DART


0.5


0.5

# Reconstructions from measured data

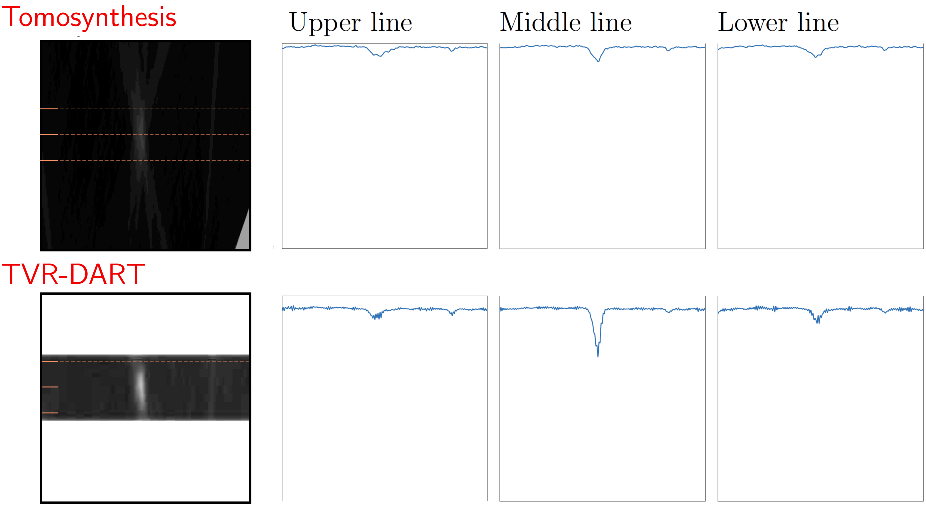


[Niemi, Salosensaari, Meaney & S, submitted manuscript]

# Outline

# Tomography appears in adaptive optics

- Modern telescope imaging suffers from turbulence in the atmosphere
  $\Rightarrow$ blurring of images
- Adaptive optics corrects the perturbed incoming light in real-time
- Major challenge in wide-field AO: atmospheric tomography

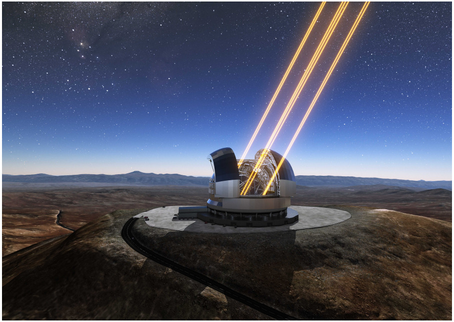

European Extremely Large Telescope (2024)

Helin, Kindermann, Lehtonen & Ramlau 2018
Yudytskiy, Helin & Ramlau 2014

# Cosmic muon imaging revealed a secret chamber inside the Pyramid of Cheops

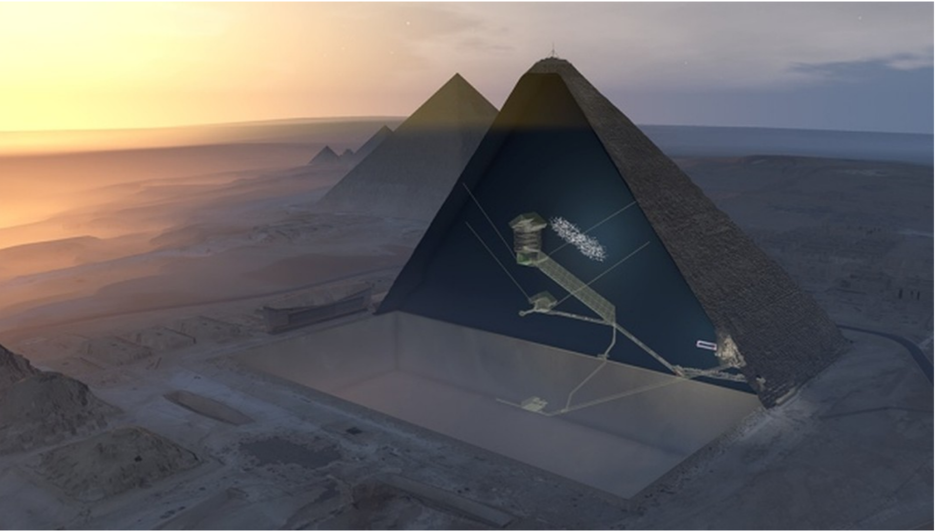

ScanPyramids

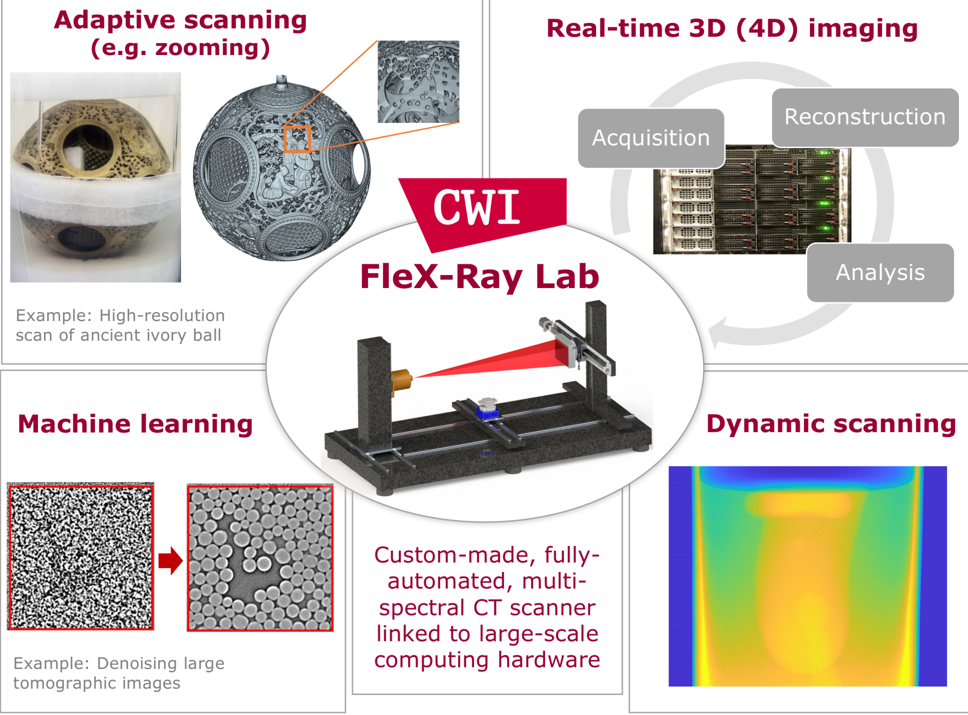
Adaptive scanning
(e.g. zooming)
Example: High-resolution scan of ancient ivory ball
Real-time 3D (4D) imaging
Acquisition
Reconstruction
Analysis
CWI
FleX-Ray Lab
Machine learning
Example: Denoising large tomographic images
Custom-made, fully-automated, multi-spectral CT scanner linked to large-scale computing hardware
Dynamic scanning

# Electron transmission cryotomography reveals the swimming engine of *Treponema primitia* bacteria

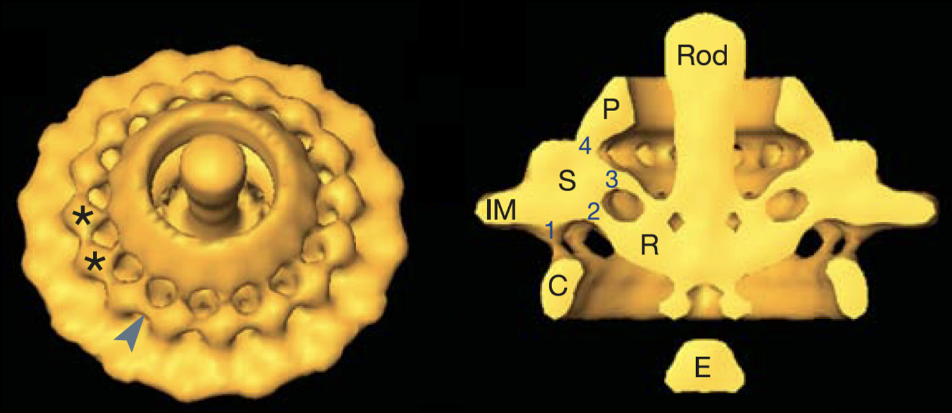


[Murphy, Leadbetter & Jensen 2016]

# University of Helsinki microtomography lab

# Links to open computational resources

Open CT datasets:

- Finnish Inverse Problems Society (FIPS) dataset page

Matrix-based parallel-beam reconstruction algorithms:
FIPS Computational Blog

- Truncated SVD
- Total Variation regularization

Matrix-free large-scale reconstruction algorithms:

- Matlab page of Mueller-S 2012 book
- ASTRA toolbox
- TVReg: Software for 3D Total Variation Regularization

# Thank you for your attention!

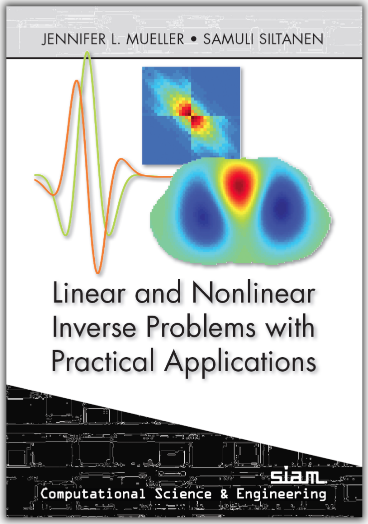


**All Matlab codes freely available at this site!**

**Part I: Linear Inverse Problems**

1 Introduction
2 Naïve reconstructions and inverse crimes
3 Ill-Posedness in Inverse Problems
4 Truncated singular value decomposition
5 Tikhonov regularization
6 Total variation regularization
7 Besov space regularization using wavelets
8 Discretization-invariance
9 Practical X-ray tomography with limited data
10 Projects

**Part II: Nonlinear Inverse Problems**

11 Nonlinear inversion
12 Electrical impedance tomography
13 Simulation of noisy EIT data
14 Complex geometrical optics solutions
15 A regularized D-bar method for direct EIT
16 Other direct solution methods for EIT
17 Projects

# Another great resource is Per Christian Hansen's 3D tomography toolbox TVreg

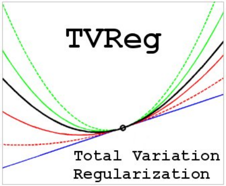


**TVreg**: Software for 3D Total Variation Regularization (for Matlab Version 7.5 or later), developed by Tobias Lindstrøm Jensen, Jakob Heide Jørgensen, Per Christian Hansen, and Søren Holdt Jensen.

Website: `http://www2.imm.dtu.dk/ pcha/TVReg/`

# These books are recommended for learning the mathematics of practical X-ray tomography

**1983 Deans:** The Radon Transform and Some of Its Applications

**1986 Natterer:** The mathematics of computerized tomography

**1988 Kak & Slaney:** Principles of computerized tomographic imaging

**1996 Engl, Hanke & Neubauer:** Regularization of inverse problems

**1998 Hansen:** Rank-deficient and discrete ill-posed problems

**2001 Natterer & Wübbeling:** Mathematical Methods in Image Reconstruction

**2008 Buzug:** Computed Tomography: From Photon Statistics to Modern Cone-Beam CT

**2008 Epstein:** Introduction to the mathematics of medical imaging

**2010 Hansen:** Discrete inverse problems

**2012 Mueller & S:** Linear and Nonlinear Inverse Problems with Practical Applications

**2014 Kuchment:** The Radon Transform and Medical Imaging